



Vaasan yliopisto
UNIVERSITY OF VAASA

Henri Hämäläinen

Development of medium voltage induction motor thermal protection function

School of Technology and Inno-
vations
Master of Science
Industrial Digitalisation

Vaasa 2020

VAASAN YLIOPISTO

Akateeminen yksikkö

Tekijä: Henri Hämäläinen

Tutkielman nimi: Development of medium voltage induction motor thermal protection function

Tutkinto: Diplomi-insinööri

Oppiaine: Industrial Digitalisation

Työn ohjaaja: DI Juha Pussinen

Työn valvoja: TKT Mohammed Elmusrati

Valmistumisvuosi: 2020 Sivumäärä: 79

TIIVISTELMÄ:

Tämän diplomityön tarkoitus on kehittää ABB:n nykyistä suojareleiden moottorin termistä suojaa. Kolmen eri kehitystavoitteen joukosta keskitytään eniten kehittämään roottorin termistä mallia, joka ottaa huomioon moottorin jättämän.

Työn teoriaosuus koostuu perehtymisestä sähkömoottoreihin, mutta erityisesti induktiomootoreihin, sekä niiden suojaamiseen. Tarkemmin perehdytään sähkömoottorin termiseen suojaan sekä ilmiöihin mitkä termisessä suojauksessa tulisi ottaa huomioon. Lisäksi työssä käydään läpi ABB:n nykyisiä sähkömoottorin termisen suojan suojafunktioita.

Olemassa olevaa kirjallisuutta hyödynnetään selvittäessä sitä, miten jättämää kyettäisiin estimoida. Lisäksi käydään läpi erilaisia toteutuksia sähkömoottorin termisen suojafunktioiden toteutuksista. Lopulta muodostetaan uusi jättämäestimaattia hyödyntävä terminen suojafunktio roottorin termistä suoja varten.

Työssä tutkitaan jättämäestimaatin laskennan toimivuutta PSCAD -simulointiohjelmistolla tuotetun datan avulla. Lisäksi simuloitua dataa muokataan erilaisten ongelmatilanteiden mukaisesti. Näin jättämäestimaatin toimivuutta testataan haastavissa olosuhteissa.

Jättämäestimaatin testausta jatketaan myös mitatun datan avulla. Näin varmistetaan estimaatin toimivuutta reaali maailman tilanteessa.

AVAINSANAT: Sähkömoottori, terminen suoja, induktiomoottori, jättämä, suojarele.

UNIVERSITY OF VAASA

Academic Unit

Author: Henri Hämäläinen

Thesis name: Development of medium voltage induction motor thermal protection function

Degree: Master of Science

Program: Industrial Digitalisation

Instructor: M.Sc. (Tech) Juha Pussinen

Supervisor: D. Sc. (Tech). Mohammed Elmusrati

Year of graduation: 2020 Pages: 79

ABSTRACT:

This master's thesis aims to develop the existing electric motor thermal protection of ABB protection relays. From the three development objectives the focus will be to develop a rotor thermal model that takes slip into account.

The theoretical part of the thesis consists of familiarization to electric motors and protecting them. The thermal protection of electric motors and the phenomena which should be taken into consideration with electric motor thermal protection are acquainted to more carefully. Additionally, the thesis will go through the existing electric motor thermal protection functions ABB has.

The existing literature will be utilized to investigate how could slip be estimated. Also, different kinds of electric motor thermal protection implementations will be discoursed. Finally, a new slip estimate utilizing electric motor thermal protection function will be formed.

The slip estimate calculation will be investigated with data produced with PSCAD simulation software. Additionally, the simulated data will be modified in order to replicate various problematic situations. This way the successfulness of the slip estimate will be tested in challenging situations.

The testing of the slip estimate will be continued with measured data. This way the successfulness can be tested with real-world circumstances.

KEYWORDS: Electric motor, thermal protection, induction motor, slip, protection relay.

Table of contents

1	Introduction	9
1.1	Background	9
1.2	Purpose and goals	9
1.3	Research plan	11
2	Three-phase electric motors	13
2.1	Definitions of three-phase and medium voltage	13
2.2	Induction motors	14
2.2.1	Construction	14
2.2.2	Basic operating principles	16
2.3	Synchronous motors	17
2.4	Operating environment	17
3	Electric motor protection	20
3.1	Basic objectives of protection	20
3.1.1	Reliability	20
3.1.2	Selectivity	20
3.1.3	Speed of operation	21
3.1.4	Simplicity	21
3.1.5	Economics	22
3.1.6	Summary	22
3.2	Potential motor threats	22
3.2.1	Overloading	23
3.2.2	Locked rotor and the skin effect	23
3.2.3	Unbalance and symmetrical components	24
3.3	Motor protection relays	25
3.4	Motor thermal protection	26
3.5	Thermal electrical relay standard	31
3.6	Thermal protection functions available in ABB protection relays	31
3.6.1	MPTTR – thermal overload protection for motor	32
3.6.2	STTPMSU – motor start-up supervision	32

3.7	Present thermal protection challenges	33
4	Mathematical modeling of slip and thermal level	35
4.1	Rotor resistance	35
4.2	Slip estimation	36
4.3	Rotor thermal model	40
4.4	Stator thermal model	43
4.5	Current ABB thermal protection	44
5	Development of the thermal protection algorithm	47
5.1	Slip dependent rotor model	47
5.2	Function proposal	47
5.3	Stator model with RTD	47
6	Evaluation of developed algorithms with a simulated motor start	48
6.1	Simulation model with PSCAD™	48
6.2	Verifying slip and thermal calculation with PSCAD™ data	51
6.3	Analyzing the function in untypical conditions	55
6.3.1	Unbalance analysis	56
6.3.2	CT saturation analysis	59
7	Field tests in Pietarsaari and testing with actual data	65
7.1	Measurement information	65
7.2	Verifying slip estimation with measured data	67
8	Conclusion	77
	References	78

Figures

Figure 1 The rotor and stator of a small three-phase induction motor (Wikipedia, 2020).	14
Figure 2 A Slip ring rotor and a squirrel cage rotor (Baradkar, 2018)	15
Figure 3 Slip ring and squirrel cage motor torque curves (Baradkar, 2018).....	16
Figure 4 Single line diagram of a power system model.	18
Figure 5 Current distribution in rotor bars caused by the skin effect (Zocholl, 2003, p. 72).	24
Figure 6 Sankey diagram of a 4 kW two-pole induction motor. P_{Fe} , iron losses; P_{Cus} , resistive losses of the stator; P_{ad} , additional losses; P_{δ} , air-gap power; P_{Cur} , resistive losses of the rotor; P_p , friction losses. (Pyrhönen et al., 2008, p. 525).....	28
Figure 7 Motor starting and thermal limit curves for a medium voltage motor.	29
Figure 8 Simulation of motor protection thermal modeling at 2 warm starts, followed by a new start after 1 hour.	30
Figure 9 Equivalent circuit model of an induction motor (Blackburn, 2006, p. 418).	35
Figure 10 Motor presented as a first-order thermal system and an electrical RC circuit (IEC 60255-149, 2013).	41
Figure 11 Rotor thermal circuit model (Zocholl, 2007).....	41
Figure 12 Stator thermal circuit model (Zocholl, 2007).	43
Figure 13 Slip-dependent thermal level calculation model. Error! Bookmark not defined.	
Figure 14 Power system model with a squirrel cage induction motor.....	49
Figure 15 PSCAD motor information configuration window.	49
Figure 16 The EMTP Type 40 format configuration window.	50
Figure 17 RMS phase currents and RMS line voltages, and simulated slip in per unit, created with the simulation tool.	51
Figure 18 Comparison between two slip estimations and one simulated slip.....	53
Figure 19 Rotor resistance factor comparison.....	54
Figure 20 Rotor thermal levels and thermal level absolute differences. θA is the thermal level for overload situation and θB is for nominal run.	55

Figure 21 Plots of positive and negative sequence components for voltage and current.	57
Figure 22 The effect of unbalance on slip estimations.	58
Figure 23 The effect of CT saturation on positive sequence current.....	60
Figure 24 The effect of CT saturation on estimated slip. The initial stator resistance defined at the 6 th power cycle.	61
Figure 25 The effect of CT saturation on estimated slip. The initial stator resistance defined after a 0.5 second calculation period.	62
Figure 26 The effect of CT saturation on the thermal levels. The initial stator resistance defined at the 6 th power cycle.	63
Figure 27 The effect of CT saturation on the thermal levels. The initial stator resistance defined during the first 0.5 seconds of the start.	64
Figure 28 A fan powered by an induction motor, at Alholmens Kraft.	65
Figure 29 Tachometer measuring the rotational speed from the motor axle.	66
Figure 30 Illustration of the measured currents, voltages and calculated slip from the tachometer measurement.	67
Figure 31 Slip comparison of the first measurement. The lower plot is a zoomed in view from the upper.	69
Figure 32 Slip comparison of the second measurement.	70
Figure 33 Slip comparison of the third measurement.	71
Figure 34 The calculated motor positive sequence resistances for each measurement. The 6 th cycle marked with a dashed line.	72
Figure 35 Comparison of the thermal levels of the first measurement.	73
Figure 36 Comparison of the thermal levels of the second measurement.	74
Figure 37 Comparison between the thermal levels of the third measurement.	75

Abbreviations

ABB	ASEA Brown Boveri
AC	Alternating current
ATEX	Explosive atmosphere

CT	Current transformer
EMTP	Electromagnetic Transients Program
FLC	Full-load current
IEC	International Electrotechnical Commission
IEEE	Institution of Electrical and Electronics Engineers
MPTR	Thermal overload protection function for motors
STTPMSU	Motor start-up supervision
RMF	Rotating magnetic field
RMS	Root-mean-square
RTD	Resistance temperature detector

1 Introduction

The purpose of this thesis is to improve ABB Distribution Solution Vaasa's (later referred to as ABB) thermal overload protection function for three-phase medium voltage induction motors.

1.1 Background

To ensure seamless and consistent operation, electric motors are protected by protective devices such as protection relays. These relays measure currents, and if needed, also voltages, to detect the abnormalities and threatening conditions.

One of the most detrimental conditions is thermal overload, which causes accelerated ageing, and can also cause insulation failures. Thermal overload can be caused by excessive mechanical overloading, which draws higher current leading into more heat generated. However, mechanically overloading the motor is still permissible for short periods of time, e.g. the motor start-up. Therefore, thermal protection must be sophisticated and accurate enough to prevent unnecessary downtime or damage to the motor.

1.2 Purpose and goals

The aim of this thesis is to develop the existing medium voltage motor thermal protection algorithm by creating two separate thermal models, one for the rotor and the other for the stator. The two key parameters that these models are to be based on are rotor slip and the direct temperature measurement from the stator windings with resistance temperature detectors (RTDs). With these models the rotor thermal behavior can be estimated more accurately, and the stator model can be biased with the temperature measurement. Together these would potentially allow more operation time and reduce the number of failed starts.

These improvements would also be able to answer to two challenges that the current thermal protection functions have. The first challenge is faced with high-inertia motor starts where the motor start-up time is close to the permissible locked rotor time, hereby making the fitting and parametrizing of the motor thermal protection difficult. Currently this challenge is answered by making some tradeoffs which decrease the level of protection.

The other challenging situation is when a motor is designed for an environment with an explosive atmosphere (ATEX rated environment). In such environments the motor must not heat excessively in order to avoid possible explosion. The motor manufacturer has therefore defined a much shorter permissible locked rotor time, even shorter than the starting time. In such an event, where starting time is longer than the permissible locked rotor time, the information whether the rotor is rotating needs to be obtained. Currently this challenge overcome by using a speed switch input to obtain the information about the rotor rotation.

There are four research questions that will be sought answers to:

1. What kinds of characteristics do three-phase induction motors have and how should these motors be thermally protected?
2. How can the motor slip be obtained?
3. How should the rotor thermal protection be done utilizing slip?
4. How should the prospective ABB thermal protection function be developed to take into account the stator direct temperature measurement?

The purpose of the first question is to gain more knowledge of the motors that are being protected as well as the relay functions that are protecting the motors. For example, it is important to know the operation principles and the environment of induction motors in order to understand how to protect them.

On the other hand, it is also valuable to understand how the motors are currently being protected. This will help to approach the algorithm development with an understanding of the ideology behind existing protection as well as from an industry standardized point of view.

The second and the third questions are related to each other as they both have a focus on slip. Slip is expected to be a parameter that will enable a more precise estimation of the rotor thermal model and therefore utilizing slip will be a focal point in the algorithm development.

The last research question is related to the stator thermal protection whereas the previous two were more focused on rotor. The last question aims to answer how to utilize the direct temperature measurement in the existing thermal protection function. The expectations for this utilization range from correcting the estimated stator thermal level values to correcting the function settings.

Ultimately this work should produce a document for ABB, based on which a new thermal protection function could be designed and implemented. The actual implementation into ABB relays will be left outside of this thesis so, that the scope of the work would not expand too much.

1.3 Research plan

The way the algorithm will be developed will consist of three areas. Firstly, getting acquainted with the necessary knowledge related to electric motors and electric motor protection, enabling a thorough understanding of the background behind the existing thermal models.

Secondly, developing the algorithm based on literature, standards and existing thermal protection functions. Widely used number computing and simulation software MATLAB® will be used to sketch, develop and also test the new thermal protection algorithm.

Lastly, the algorithm will be tested in order to validate that it works properly and to analyze its reliability and sensitivity. The testing will be done with simulated and measured data. A power system simulation software, PSCAD™, will be used to obtain the simulated data. This data will be used for the first tests for the algorithm, including tests how the algorithm works in measurement affecting conditions such as current unbalance and when the current transformer saturates. The measured data will be obtained from an actual three-phase medium voltage induction motor located at Alholmens Kraft Pietarsaari. The measured data should confirm that the algorithm in fact works in real-life situations.

2 Three-phase electric motors

Electric motors are widely used in industrial applications, and according to a study by Bazurto et al. (2016) electric motors consume approximately 68% of the electricity worldwide in the industrial sector. Therefore, it is important to maintain high efficiency and reliability when it comes to electric motor operation.

Electric motors are popular as industry and transportation workhorses. While the largest electric motors can be used for ships' propulsion, the more common usages are powering fans, blowers and pumps. The popularity of electric motors can be explained by their efficiency and price, but also their convincing torque range which allows them to be used in all kinds of applications.

The three-phase electric motors can be divided into two main categories, induction motors i.e. asynchronous motors, and synchronous motors. There are also various types of motors in both main categories. In induction motors there are squirrel cage and slip ring motors i.e. wound rotor motor, and in synchronous motors there are non-excited and DC-excited motors. This thesis will focus on induction motors, squirrel cage motor in particular.

2.1 Definitions of three-phase and medium voltage

As the thesis is about three-phase medium voltage induction motors, it seems appropriate to clarify the definitions of these terms.

Three-phase electric power is a definition related to alternating current (AC). In the context of electric power systems, in which electric motors are also included, three-phase electric power means that the current is carried in three different conductors, each having AC current flowing through them. Ideally the currents are equal in amplitude, but each phase is separated by 120 degrees from one another.

The other term, medium voltage, refers generally to voltages between 1 and 35 kilovolts. However, with motors the range is typically between 1 and 11 kilovolts. The definition of the range is a bit vague since it depends on how each operator wants to define it.

2.2 Induction motors

2.2.1 Construction

An induction motor, alike any electric motor, consists of two main assemblies, stator and rotor (Figure 1). The stator is the stationary unit, consisting of windings placed in the slots of a laminated steel core. The rotor is the rotating unit, which has a cylindrical core consisting of steel laminations and, in a squirrel cage induction motor, aluminum bars which are mounted near the surface of the rotor. The rotor of other types of electric motors differs from the description above, but the stator is very similar. (Herman 2011, p. 522)

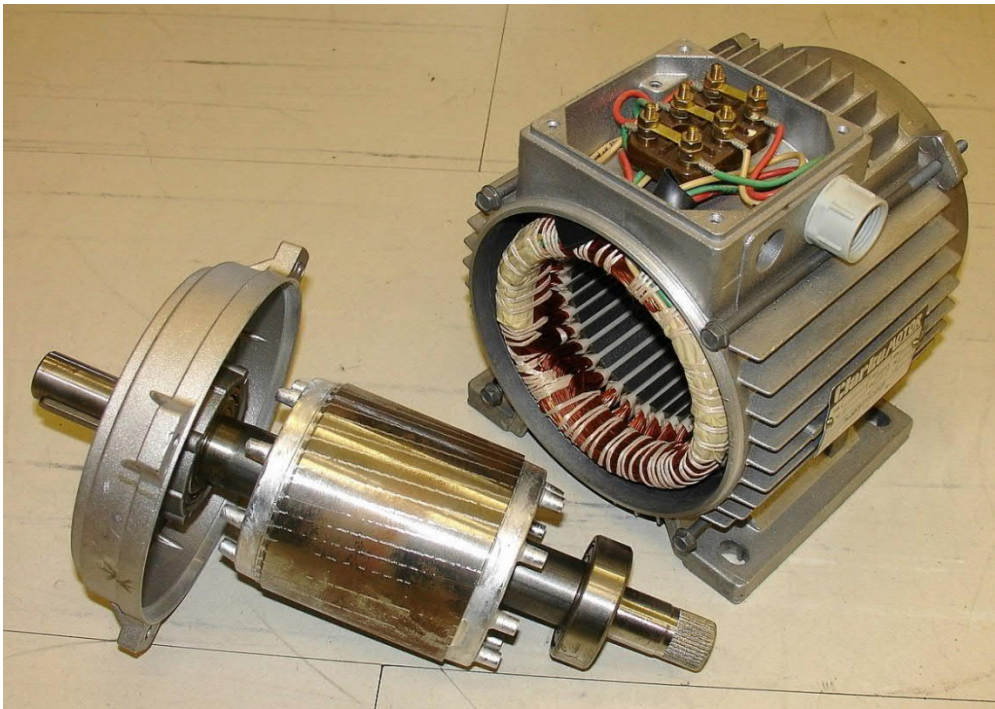


Figure 1 The rotor and stator of a small three-phase induction motor (Wikipedia, 2020).

Figure 2 illustrates the rotational part of slip ring and squirrel cage motors. Compared to the squirrel cage rotor, which is quite bare, the slip ring rotor has windings and slip rings.

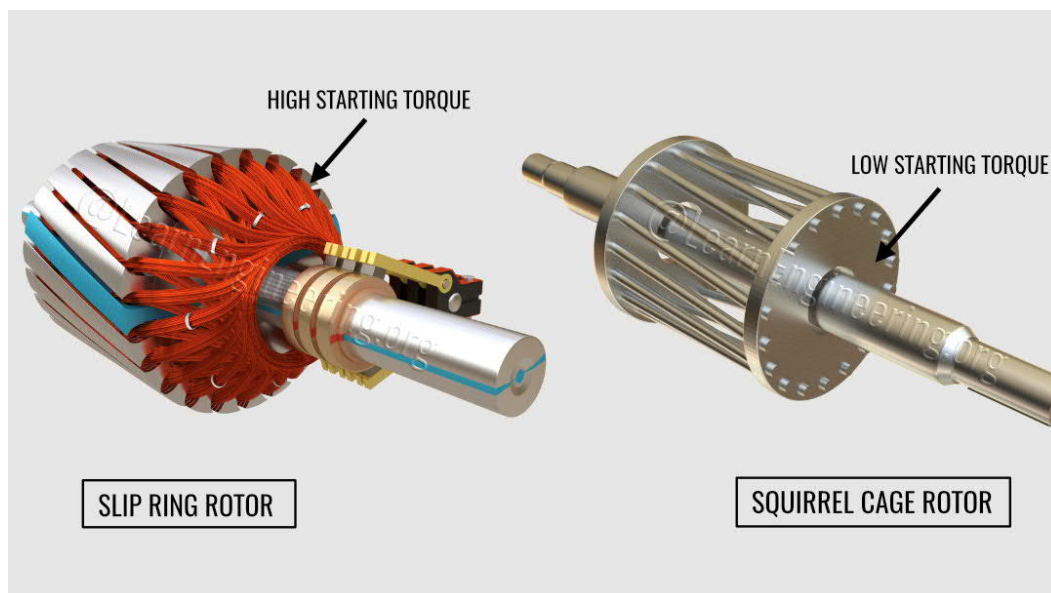


Figure 2 A Slip ring rotor and a squirrel cage rotor (Baradkar, 2018)

The slip rings provide external resistances connected in series with the rotor windings that allow the motor to have high, adjustable torque throughout its speed range. This quality makes slip ring motors have different usages compared to squirrel cage motors. Slip ring motors are often used for lifts, elevators and compressors, when high starting torque is required (TECO-Westinghouse, 2019). The drawback for the slip ring motors of having great adjustability with the starting torque is that the building and maintenance costs are higher than the rather simple structure of the squirrel cage motor. It is a tradeoff between versatility and costs.

Squirrel cage motors on the other hand, tend to have a lower starting torque but a high peak torque close to the motors nominal speed (Figure 3). Hence, squirrel cage motors are best in applications that maintain constant speed and desire low maintenance. These applications include centrifugal pumps, industrial drives and large blowers and fans.

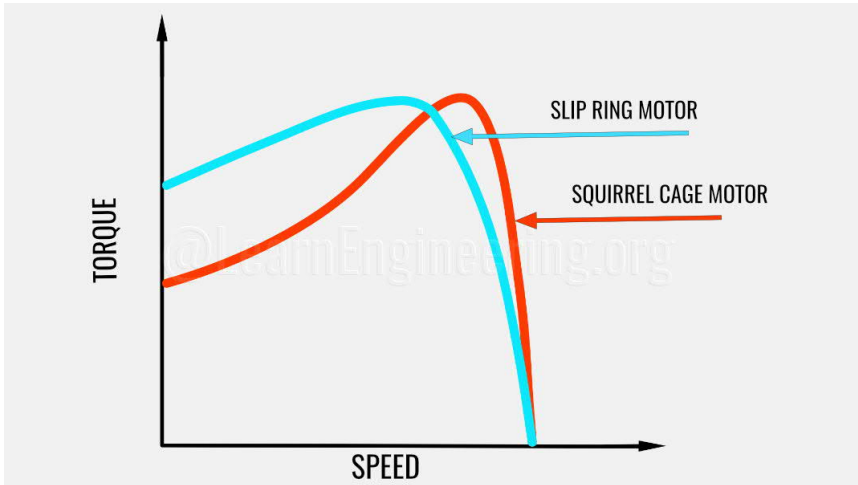


Figure 3 Slip ring and squirrel cage motor torque curves (Baradkar, 2018)

2.2.2 Basic operating principles

When driving an electric motor, the magnitude of the stator current that is drawn from the power network by the motor at full speed is predetermined by the motor manufacturer. This rated current, also known as the full load current, is the stator current that the motor draws at the rated voltage and when the motor is running with nominal i.e. full load.

The rotor is made to rotate with a rotating magnetic field (RMF) created by the currents flowing in the stator windings. With squirrel cage rotors, when the field rotates, it cuts through the rotor aluminum bars, inducing current to them. This current then creates its own magnetic field, which in connection to the RMF creates a mechanical force that makes the rotor rotate.

As the rotor rotational speed increases, the induced current and its frequency become smaller (Korpinen, 1998). In fact, if the rotor were to reach the speed of the RMF i.e. synchronous speed, the RMF would not cut the rotor bars, hence no current would be induced. This makes it so that the synchronous speed is not able to be maintained and the rotor lags slightly behind the RMF. The amount of the lag i.e. the relation between

the rotor speed and the synchronous speed is called the slip. Slip is calculated from the rotor speed and synchronous speed as follows:

$$Slip = 1 - \frac{Rotor\ speed}{Synchronous\ speed} \quad (1)$$

In induction motors slip values vary between one and zero. Slip is one when the rotor is not moving, and as the rotor starts gaining speed the slip values approach but do not quite reach zero.

2.3 Synchronous motors

Similar to induction motors, synchronous motors are also made to rotate by the stators RMF. However, the rotor is rarely induced when running at full speed. Commonly the rotor consists either of permanent magnets or electromagnets i.e. windings that are fed with current. This means that the stator RMF is able to rotate the rotor at synchronous speed, since no induction is needed.

Yet some synchronous motors can also utilize induction. Large synchronous motors can include a separate squirrel cage induction assembly, called the damper winding, in order to have sufficient amount of torque to accelerate. (WEG Group, 2012, p.3) Thus, those motors can be started as induction motors and after closing in on the synchronous speed, the rotor windings are fed current in order to then close out the slip and maintain the synchronous speed.

2.4 Operating environment

Power systems are often composed of multiple various electronic components such as the electric motor, distribution lines, transformers as well as the protection relays. In order to understand what kind of environment electric motors and protection relays are usually operated in, a simplified model can be used.

Figure 4 illustrates a single line diagram of a power system, focusing on a single electric motor and the protection relay. In the single line diagram, the three phases are represented as a single line to simplify the drawing.

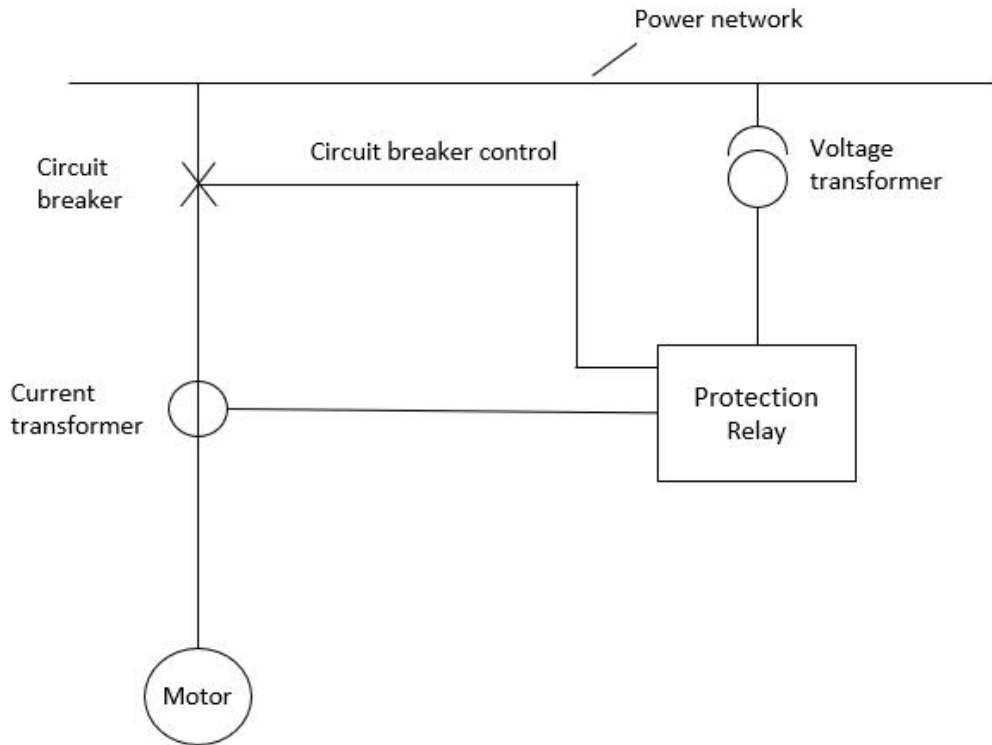


Figure 4 Single line diagram of a power system model.

Figure 4 shows a typical way the motor, current and voltage transformers as well as the protection relay are connected. This illustration gives information about what the relay measures in the power system. The currents that the relay measures are the secondary currents from the current measuring transformer, connected to the motor feeding cable.

The voltages and currents going to the motor are relatively high, whereas the currents and voltages the protection relays are able to measure need to be quite low. Thus, measuring transformers are needed to change the currents and voltages suitable for the sensitive protection relays.

When protecting medium voltage devices, the current measurement is the most common single measurement. The possible abnormalities in the measured signal can be traced to the current transformer. In case the transformer primary side current is multiple times larger than the transformers nominal current, the transformer will saturate. If the current transformer saturates notably, the measured sinusoidal signal is distorted by harmonics, making the calculations done based on this measured current suffer (Blackburn & Domin, 2006, p. 184).

In conclusion, the knowledge of the common measurement connections is helpful in order to understand what kind of things affect the measured signals. This makes it easier to identify and analyze situations where disturbances occur. The motor start is the most crucial situation since the current drawn by the motor are at their highest.

3 Electric motor protection

This chapter covers the basic objectives of protection, common faults and electric motor protection in general. It also covers motor thermal protection in general as well as the overview and challenges of the motor thermal protection functions ABB uses.

3.1 Basic objectives of protection

Five key terms describe and shape basic objectives of protection (Blackburn & Domin, 2006, p. 48):

1. Reliability
2. Selectivity
3. Speed of operation
4. Simplicity
5. Economics

3.1.1 Reliability

The first term reliability has two aspects, dependability and security. Both aspects have IEEE standardized definitions. Dependability is achieved by maximizing the probability that a fault will be reacted to with a correct protective action. Security is very closely related to the dependability, as it is achieved by minimizing the probability that there is an incorrect operation. Simply, dependability tries to ensure that faults are reacted to and security tries to ensure that no unnecessary reactions occur (Blackburn & Domin, 2006, p. 49).

3.1.2 Selectivity

Power grids often have multiple protection relays assigned for each area or component in the grid. As the grid is divided into smaller zones, a detected fault can be reacted to in such a way that only the zone in which the fault is located in is disconnected i.e. de-energized. This makes it so that the disconnect effects only on the minimum area

necessary, enabling the rest of the grid remain energized. For example, a fault in the motor would only disconnect the motor from the grid rather than the whole grid the motor is connected to.

3.1.3 Speed of operation

A fast or instantaneous reaction is in theory, always coveted. Nevertheless, some applications might suffer from overly fast operating times, as some faults might require some time to be correctly identified. Although, operating, even too hastily, can be yet considered just since it means that the protection is dependable. However, in such cases the security aspect suffers, but it is important to note that in the real-world it is often better to be on the safe side.

3.1.4 Simplicity

In Blackburn's and Domin's (2006, p?) book, *Protective Relaying*, simplicity is described as follows: "A protective relay system should be kept as simple and straightforward as possible while still accomplishing its intended goals." Simplicity is an objective that assumes that the real-world is not ideal. Trying to accomplish protection that is too intricate and complicated can lead to more harm than gain. For example, the protection relays are designed with certain amount of processing power, therefore also limiting the protection functions' level of complexity. For example, a finite element model of the motors thermal behavior would be overly complex for the relay in terms of processing power as well as protection-wise. Additionally, simplicity can mean faster speed of operation, allowing to aim for two goals at once.

Additionally, simplicity is also a quality which alleviates the configuration of the protection relay for the customer. Protection functions that have too intricate settings can be unnecessarily difficult for the customer to configure properly.

3.1.5 Economics

The saying “good does not come cheap” can be also used when discussing about basic protection objectives. Thereby, it could be presumed that the lowest-priced protection system might not be the most reliable, adequate or user friendly one. These products are often not as well tested or built either. Therefore, it is important to understand that although a low-cost protection system might seem like a good idea to save money initially, it might come to be a costly decision on the long term. This is because in case the protection fails and the protected equipment suffers damage, the maintenance and repair costs are much higher than the cost of a proper, slightly more expensive protection.

3.1.6 Summary

The basic objectives of protection define a good guideline which to follow but in the actual implementation will most likely always have some sort of simplification or tradeoffs. Real-world circumstances make it ludicrous to assume that perfect protection would always be achieved. Nevertheless, it does not mean that it should not be pursued. It is the responsibility of the protection engineer to balance the objectives and optimize the protection situationally.

3.2 Potential motor threats

Electric motors are vulnerable to various conditions that can either cause a shutdown or actual damage to the motor. Here is a list of conditions that are considered hazardous for induction motors (Blackburn & Domin, 2006, p. 415):

1. Phase and ground faults
2. Excessive thermal overloads
 - a. Overloading (continuous or intermittent)
 - b. Locked rotor (failure to start or jamming)
3. Abnormal conditions
 - a. Unbalance
 - b. Under- and overvoltage

- c. Reversed phases
- d. High-speed reclosing
- e. Unusual ambient conditions
- f. Incomplete starting sequence

For this study, the excessive thermal overloads are the most pivotal. Additionally, even though unbalance is classified as an abnormal condition, it can also cause excessive thermal overloading.

3.2.1 Overloading

Mechanical overload and thermal overload are two separate things that might cause confusion. While thermal overload is always detrimental for the motor, mechanical overloading is not. For example, electric motors can be mechanically overloaded for a certain amount of time. In such case the motor draws more current from the grid, making the motor heat up more. The motor can be mechanically overloaded for even relatively long periods of time depending on the amount of overload applied, until the motor reaches the estimated thermal overload limit, resulting in the relay tripping i.e. disconnecting the motor by opening the circuit breaker.

Each electric motor has its thermal limits based on the insulation class defined to the motor. Exceeding this thermal limit, even for short periods of time, can damage the motor and shorten its life-expectancy.

3.2.2 Locked rotor and the skin effect

Locked rotor describes a situation where the rotor is unable to rotate. An example of this is a situation where the mechanical torque produced by the motor is smaller than the mechanical load, making the rotor unable to rotate. This condition occurs commonly during motor start-up, especially with high-inertia motors. However, it can also occur

whilst the motor is running if the mechanical load applied is increased, or if motor torque drops for any reason.

When the rotor is locked, the stator RMF cuts the rotor bar with the grid frequency inducing a high amplitude and a relatively high frequency current. When a high frequency alternating current flows in a cylindrical structure such as the rotor bar, the current tends to distribute so, that the current density is highest close to the surface of the bar (Zocholl, 2003, p. 71). The occurrence of this distribution is called the skin effect. The distribution differences are illustrated in Figure 5, where the positive sequence current distribution is on the left and negative sequence current is on the right. Locked rotor condition should also produce similar distribution as negative sequence current which is introduced in the next subchapter.

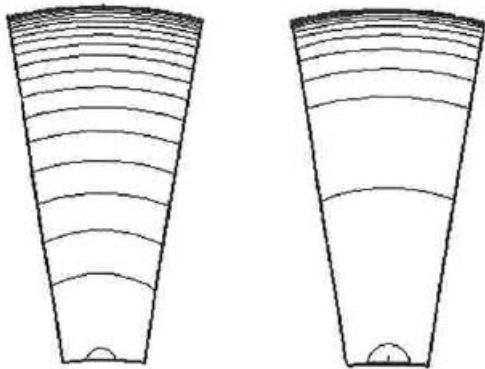


Figure 5 Current distribution in rotor bars caused by the skin effect (Zocholl, 2003, p. 72).

The skin effect increases the rotor bar resistances which causes very rapid heating of the rotor, further increasing the rotor bar resistances. The increase in resistance depends on the relation between the stator RMF and rotor speed.

3.2.3 Unbalance and symmetrical components

In general, unbalance is a condition where the three-phase stator currents are either unequal in magnitude or not separated from each other by exactly 120 degrees. Differing

from the ideal situation, where there is only a positive sequence component, also a negative sequence component exists. Unbalance situation occurs commonly with an open phase but abnormalities in the power grid can also cause unbalance.

In order to understand unbalance and its effects on induction motors, a method of symmetrical components is used. With induction motors, symmetrical components are used to describe and analyze the effects that the input currents and voltages have. Essentially, symmetrical components consist of three different sets: positive, negative and zero sequence.

Positive sequence component creates a force that rotates the rotor in the intended direction. The negative sequence component being the opposite to this, tries to force the rotor in the unintended direction. Zero sequence component effect on the rotor rotation is negligible.

The magnetic flux that the negative sequence current creates rotates in the opposite direction compared to the intended direction of the rotor rotation. The effect of unbalance can be seen in the rotor current frequency (Blackburn & Domin, 2006, p. 428). The current frequency depends on the rotor rotational speed. In a locked rotor condition unbalance does not affect the rotor current frequency, but when the motor is running at full speed the induced current frequency is doubled. Due to skin effect, this causes the rotor to heat extremely rapidly (Zocholl, 2003, p. 72).

3.3 Motor protection relays

Protection relays are used to protect electrical components and devices from various detrimental conditions and phenomena. The electrical components and devices can be for example motors, generators or feeders etc. This thesis will concentrate on the protection of induction motors, and more specifically, the thermal protection of the motor.

ABB Relion® protection relay series consists of products that are able to protect multiple different equipment. The Relion® relays have capabilities to protect, control, measure and supervise power systems with different kinds of functions. The desired functions are selected based on the protected object and they are configured according to the demands that the equipment manufacturer has set.

The newest relay in the Relion® series is the REX640, which is a protection and control relay that can be utilized in many different power distribution and generation applications, making it stand out from the older relays with its versatility. It is a high-end protection and control relay and the flagship model in the Relion® protection relay series.

The relay functions are configured according to the equipment at hand. To protect the equipment correctly, the functions need information about the motor, which can be obtained for example from the motor nameplate or, if available, a motor data sheet. The more information available, the better the protection.

3.4 Motor thermal protection

Thermal protection has a crucial role in protecting the motor as thermal overload is one of the most detrimental conditions for the motor due to the damage it causes to the motor. Moreover, motor start-ups are especially essential since the motor heats up extremely fast due to the starting currents being multiple times higher than the full load current. In the start-up situations, both the stator and rotor deal with high currents but the heating of the rotor is more significant due to the skin effect mentioned before.

Thermal overload limits the use of the motor and thermally overloading the motor deteriorates the insulation. This shortens the motors lifetime and ultimately, as the insulation fails, causes an electrical fault, and might even melt the windings.

The rapid heating during the start-up limits the amount of consecutive starts. Usually the motor manufacturer declares the number of consecutive starts, ranging from 2-3 cold

starts or 1-2 warm starts. Cold start is defined as a start where the motor temperature at the time of first start is the same as the motor ambient temperature. A warm, or a hot start occurs when the motor is started, and it has been run on its designed operational temperature.

The motor heat is produced from motor losses, which exist because the motors are not ideal. The losses are classified as follows:

- Resistive losses i.e. copper losses in stator and rotor conductors.
- Iron losses in the magnetic circuit.
- Additional losses.
- Mechanical losses.

Figure 6 represents an example of an enclosed 4kW induction motor and the relative percentual losses (Pyrhönen et al., 2014, p. 525). In this example, 15% percent of the electrical energy will be converted into heat at the rated power of the motor. Most of these losses (11.6%) are resistive losses in stator and rotor conductors.

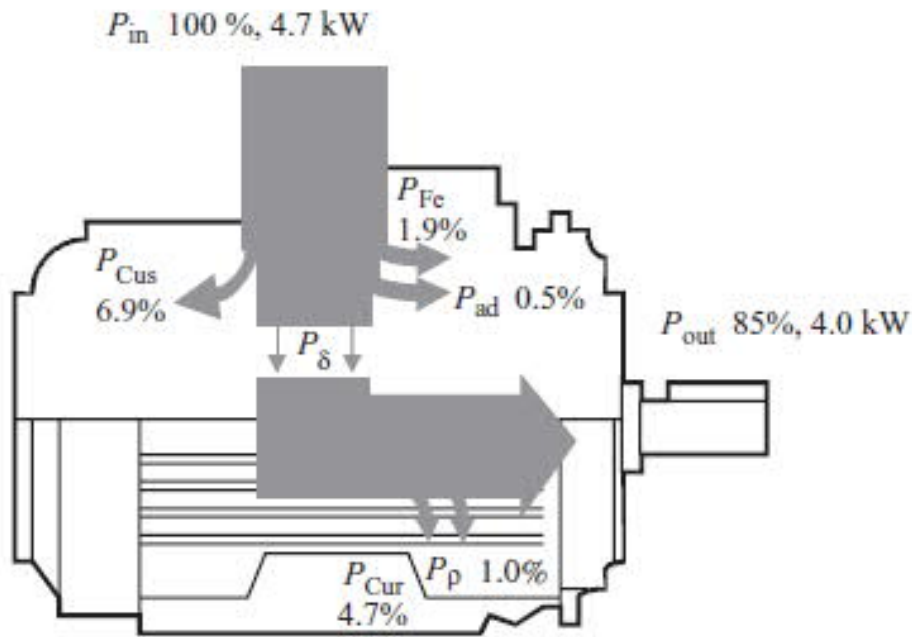


Figure 6 Sankey diagram of a 4 kW two-pole induction motor. P_{Fe} , iron losses; P_{Cus} , resistive losses of the stator; P_{ad} , additional losses; P_{δ} , air-gap power; P_{Cur} , resistive losses of the rotor; P_p , friction losses. (Pyrhönen et al., 2008, p. 525)

The resistive losses are mathematically described by a formula, and the same principle is also implemented in thermal protection functions:

$$P = I^2 * R, \quad (2)$$

where P is the heat loss in watts,
 I is the current in amperes and
 R is the stator and rotor winding resistances in ohms.

To effectively protect the motor against thermal overload, the protection relay should have a thermal model of the motor. The thermal model continuously calculates an estimation of the thermal level of the motor. The thermal relay trips if the allowed maximum thermal level is reached.

When designing motor thermal protection, trip time curves are used to fit the protection function while taking into consideration the motor manufacturers demands. These demands must be met in order to enable the amount of motor use the motor manufacturer has promised. Figure 7 illustrates trip time curves for a certain induction motor. This specific case presents a challenge for the motor protection. The motor current curves are relatively close to the hot and cold thermal limit curves defined by the motor manufacturer. The closer to each other these curves are the more difficult it becomes to fit the relays trip time curves in between to provide sufficient protection. This kind of situation is common with high-inertia motors.

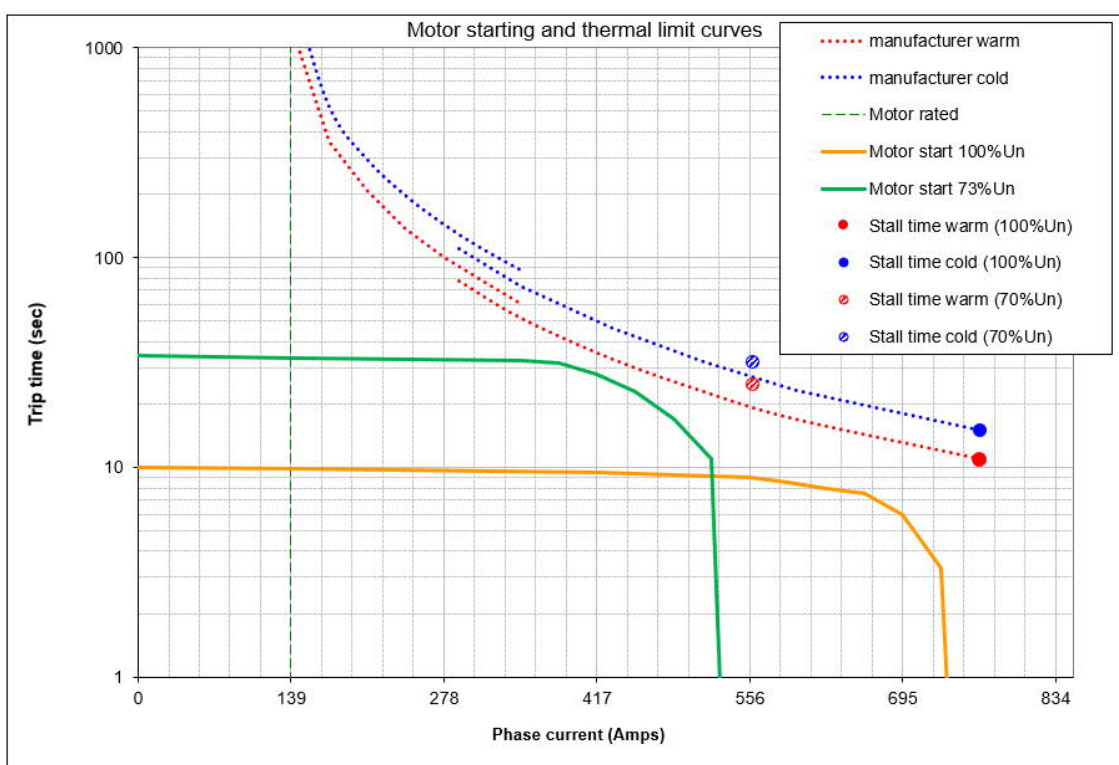


Figure 7 Motor starting and thermal limit curves for a medium voltage motor.

An even more difficult situation to set the protection functions is when the permissible locked rotor time is less than the starting time of the motor. Since the rotor is considered to be locked during the start, this proposes a challenge that is impossible to overcome without the information that the rotor has started rotating. This information can be obtained two different ways. Either the motor has to have a speed switch which indicates

that the rotor has started rotating or an impedance protection is used. The impedance protection i.e. distance protection calculates the motor impedance from the input voltage and current. The calculated impedance values increase in magnitude and change in phase angle as the motor accelerates, which enables to determine that the rotor has started rotating (Blackburn & Domin, 2004, p. 427).

Although setting trip time curves already provide challenging constraints, the protection function must also fulfill the motor manufacturers demands in the amount of cold and hot starts allowed. In order to demonstrate that these demands are met, thermal simulation curves of motor starts are used. The simulation curves show the calculated thermal level of the protected motor (Figure 8). Theta-A represents the hotspot thermal level, which reaches high peaks. Theta-B represents the longer-term thermal level, depicting components with more stable thermal rise.

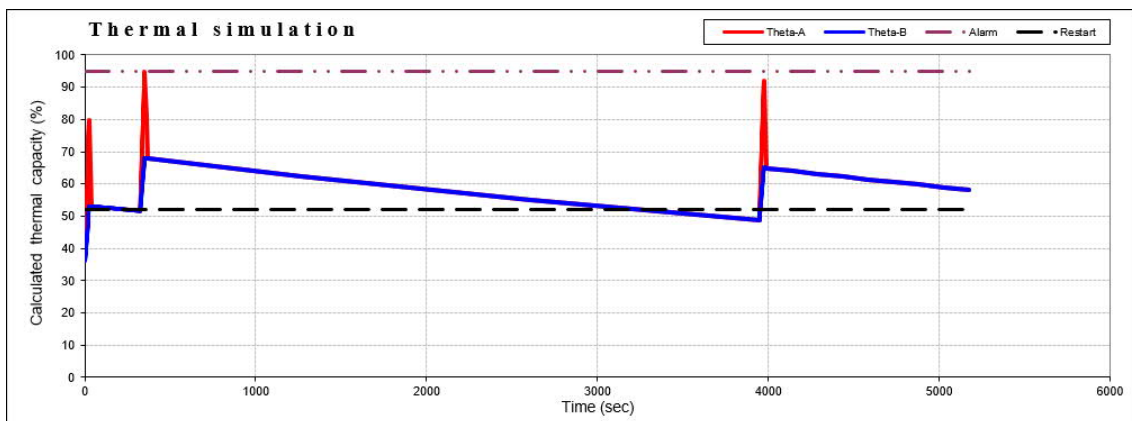


Figure 8 Simulation of motor protection thermal modeling at 2 warm starts, followed by a new start after 1 hour.

In order to fulfill the motor manufacturers demands, the motor must be allowed a certain amount of consecutive hot and cold starts, as mentioned earlier in this subchapter. For example, Figure 8 illustrates a simulation allowing two consecutive starts for a hot motor. And if the motor was stopped, it would be possible to be restarted after about a one-hour cooldown time.

In conclusion, the parametrization of the protection relay should allow the user to set the protection functions so, that both the motor thermal limit curves, and the consecutive start demand are met. However, situations such as high-inertia motor starts make the protection function parametrization difficult or even impossible. This means that the protection function cannot be set to match the motor manufacturers demands unless a speed switch or an impedance protection is used. Otherwise sufficient protection is also difficult to offer.

3.5 Thermal electrical relay standard

IEC 60255-149 is the standard that sets functional requirements for thermal electrical relays. It specifies the minimum requirements for thermal protection relays, such as a simple first-order thermal model of electrical equipment based on which the thermal level calculations are done. The aim of the standard is to establish a common and reproducible reference for relays that protect equipment from thermal damage by measuring alternating currents flowing through the equipment (IEC 60255-149, 2013).

This standard provides the background for the existing thermal protection function. It helps to understand the boundaries in which the thermal protection should work in.

3.6 Thermal protection functions available in ABB protection relays

ABB has two separate protection functions, thermal overload protection for motors (MPTTR) and motor start-up supervision (STTPMSU), that are used together to provide thermal protection to electric motors. MPTTR is used specifically for motor thermal protection, whereas STTPMSU is a collection of functions which are used to supervise motor start-up.

3.6.1 MPTTR – thermal overload protection for motor

MPTTR is a thermal protection function for motors that is based on measured currents. The function is focused on the protection of the stator, but it also takes into account hotspots which the rotor is recognized as.

MPTTR protects electric motors from overheating. It models the thermal behavior of the motor based on the measured load current and disconnects the motor if the motor calculated thermal level reaches 100 percent.

The thermal overload is the most often encountered abnormal condition in industrial motor application, which emphasizes the importance its protection (ABB Oy, 2019, p. 387). MPTTR protects an electric motor from the phenomena such as the premature insulation failures of the windings by preventing the motor from drawing excessive current and overheating.

3.6.2 STTPMSU – motor start-up supervision

STTPMSU is a function that consists of four different modules: start-up supervisor, cumulative start-up protection, thermal stress calculator and stall protection. The main purpose of this function is to protect the motor against prolonged starting time, excessive number of starts and the locked rotor condition during start-up.

From the aforementioned four modules, thermal stress calculator and stall protection are the ones of interest for this thesis.

The thermal stress calculator prevents the motor from overheating during the motor start-up. It calculates the thermal stress imposed on the rotor during the start-up and compares it to the thermal stress limit defined by the motor starting current and permissible starting time. If the calculated value reaches the limit, the relay trips.

Stall protection module protects in such cases where the motor stalling time is shorter or close to the starting time. It must then receive a signal from the motor speed switch indicating that the rotor has started revolving, otherwise the relay will trip.

It is worth to note that where MPTTR has a thermal memory, STTPMSU does not. Both thermal stress protector and stall protection reset after the start-up ends or if the relay trips.

3.7 Present thermal protection challenges

Current challenges with the MPTTR and STTPMSU functions occur in quite specific situations. Those two situations, as mentioned in the introduction, are high-inertia motor start-ups and start-up protection for motors designed for an environment with an ATEX classification.

The high-inertia motor starts are currently dealt with precise parametrization of the protection function. In rare cases, this method might fail to answer to the motor manufacturer's, or the motor protection demands, and more commonly makes the parametrization tedious for the customer.

Motors that are designed for ATEX classified environments are not allowed to reach high temperatures. Often the highest temperature values are reached during start-up, since the current is multiple times higher than while running, and the temperatures rises especially if the rotor gets locked. Therefore, motor manufacturers have defined permissible locked rotor times that are lower than the starting times.

With these kinds of motors, the challenge is not so much in the parametrization, whereas it lies with getting the information that the rotor has started rotating. In these situations, the protection function must receive this information within the permissible locked rotor time. The information is currently received from a speed switch. However, motors that are reliant on the rotor revolution indication do not always have a speed switch.

The existing thermal protection functions are reliant on the speed switch to detect the rotor rotation. If a speed switch is not present it is impossible to get the motor running unless the protection is compromised by changing the thermal protection function values.

In conclusion, these challenges are currently met with solutions that are tedious and difficult for the customer and might often require tradeoffs. Also, seldomly a solution providing sufficient protection can be unavailable. A simpler solution would save the customer a lot of effort and also guarantee better protection for the motor.

4 Mathematical modeling of slip and thermal level

This chapter will describe the mathematics and equations that are found in the existing literature. It explains a way to estimate motor slip and two different ways to calculate the thermal level.

In the literature the slip-dependent rotor thermal model uses two main formulas, one to calculate the slip, and the other to calculate the rotor thermal level. The latter formula is divided into two slightly different formulas depending on the amplitude of the motor current. The formulas require various parameters that are either obtained from the manufacturer's data or calculated from them (Zocholl, 2007).

An important base for the modeling the rotor thermal level is the Steinmetz's equivalent circuit model of an induction motor (Figure 9). This circuit is used to derive the equations for calculating rotor resistance and estimated slip.

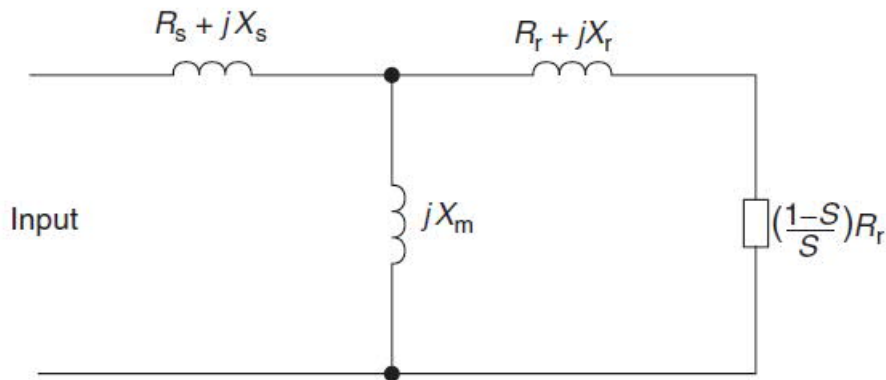


Figure 9 Equivalent circuit model of an induction motor (Blackburn, 2006, p. 418).

4.1 Rotor resistance

The change in rotor resistance is a defining characteristic for the rotor thermal level equation. As can be seen from the Equations 3 and 4, that are derived from the Steinmetz's equivalent circuit model, the rotor resistance is assumed to change linearly

depending on the slip. These equations describe the change in rotor resistance relative to the motor speed due to the skin effect (Zocholl, 2003, p. 30).

$$R_{r+} = (R_L - R_N) * S + R_N, \quad (3)$$

$$R_{r-} = (R_L - R_N) * (2 - S) + R_N, \quad (4)$$

where R_{r+} is the rotor positive sequence resistance,
 R_{r-} is the rotor negative sequence resistance,
 R_L is the locked rotor resistance,
 R_N is the rotor resistance at nominal speed and
 S is the motor slip.

Equation 3 receives the highest values when the rotor is locked. In a stall situation, the rotor resistance is trifold, and the starting torque is also larger (Pyrhönen et al., 2018). As the rotor speed gradually catches up to the RMF speed, the resistance decreases as the skin effect diminishes.

Equation 4 however reaches its highest values when the motor is running at rated speed. This is due to the fact that if there were a negative sequence RMF, it would rotate in the opposite direction compared to the rotor, therefore inducing a current with very high amplitude and frequency to the rotor. The rotor resistance values can at that time reach five times the value compared to rotor resistance at rated speed. (Zocholl, 2007)

4.2 Slip estimation

An early objective for this thesis was to develop a rotor thermal model based on slip. Now, if it was possible, slip could be measured from the rotor axle, but this possibility is unlikely to be available. Therefore, slip has to be estimated from signals and parameters measured or obtained from the motor.

There is a series of patents regarding rotor thermal model, in which the slip is estimated based on the sampled currents and voltages as well as some other parameters specific to the motor. Additionally, the author of these patents, Stanley E. Zocholl had published papers and a book discussing about AC motor protection in general as well as the slip-based rotor thermal model.

The equation estimating slip is derived from the Steinmetz's equivalent circuit model. The estimated slip is a particular solution of the equation for motor apparent positive sequence impedance.

The apparent positive sequence impedance can be calculated from the positive sequence current and voltage:

$$\vec{Z} = R + jX = \frac{\vec{V}_1}{\vec{I}_1} \quad (5)$$

where \vec{Z} is the motor positive sequence impedance,
 R is the motor positive sequence resistance,
 X is the motor positive sequence reactance,
 \vec{V}_1 is the positive sequence voltage and
 \vec{I}_1 is the positive sequence current.

The same positive sequence impedance can also be formulated from the Steinmetz's equivalent circuit model:

$$\vec{Z} = R_S + jX_S + \frac{(\frac{R_r}{s} + jX_r) \times jX_m}{\frac{R_r}{s} + jX_r + jX_m} \quad (6)$$

where R_S is the stator positive sequence resistance,
 X_S is the stator positive sequence reactance,
 R_r is the rotor positive sequence resistance,

S is the motor slip,
 X_r is the rotor positive sequence reactance and
 X_m is the magnetizing reactance.

Further expanding the equation:

$$\vec{Z} = R_S + jX_S + \frac{\frac{R_r X_m^2}{S} + j(X_m \left(\frac{R_r}{S}\right)^2 + X_r X_m (X_r + X_m))}{\left(\frac{R_r}{S}\right)^2 + (X_r + X_m)^2} \quad (7)$$

Now focusing only on the real part of impedance:

$$R = R_S + \frac{\frac{R_r X_m^2}{S}}{\left(\frac{R_r}{S}\right)^2 + (X_r + X_m)^2} \quad (8)$$

The equation can be arranged so that a part that is found negligible can be removed to simplify the equation (Zocholl, 2007):

$$R = R_S + \frac{\frac{R_r}{S}}{\left(\frac{R_r}{S}\right)^2 \frac{1}{X_m^2} + \frac{(X_r + X_m)^2}{X_m^2}} \quad (8)$$

Here $\left(\frac{R_r}{S}\right)^2 \frac{1}{X_m^2}$ is the negligible part. Also, $\frac{(X_r + X_m)^2}{X_m^2}$ is further denoted as A , resulting in:

$$R = R_S + \frac{R_r}{A \times S} \quad (10)$$

Then replacing the R_r with Equation 3, slip is calculated as follows:

$$S = \frac{R_N}{A \times (R - R_{SI}) - (R_L - R_N)} \quad (11)$$

where S is the motor slip,
 R_N is the rotor resistance at rated speed,

A is a reactance constant,

R is the motor positive sequence resistance,

R_{SI} is the initial stator positive sequence resistance and

R_L is the rotor resistance locked rotor.

In Equation 11 all other parameters except R are constants, and per unit values, that can be either obtained or calculated from the motor data. The motor positive sequence resistance R is calculated as such (Zocholl, 1990, p.5):

$$R = \text{real}\left(\frac{\vec{V}_1}{\vec{I}_1}\right) \quad (12)$$

where \vec{V}_1 is the positive sequence voltage and

\vec{I}_1 is the positive sequence current.

Another way to calculate R is directly from the phase currents and voltages:

$$R = \text{real}\left(\frac{\vec{V}_A}{\vec{I}_A} + \frac{\vec{V}_B}{\vec{I}_B} + \frac{\vec{V}_C}{\vec{I}_C}\right) / 3 \quad (13)$$

where $\vec{V}_A, \vec{V}_B, \vec{V}_C$ are the phase voltages and

$\vec{I}_A, \vec{I}_B, \vec{I}_C$ are the phase currents.

Equation 11 also has some parameters that can be calculated in different ways. For example, the initial stator resistance R_{SI} has three different ways found in the literature.

First, the way that the Zocholl patent (1990) states: $R_{SI} = R_P - \frac{R_L}{A}$, where R_P can be calculated as $R_P = \text{real}\left(\frac{\vec{V}_{1(cyc)}}{\vec{I}_{1(cyc)}}\right)$, where $\vec{V}_{1(cyc)}$ and $\vec{I}_{1(cyc)}$ are the positive sequence voltage and resistance after a short settling period somewhere between 1-8 power cycles,

or $R_P = \text{real}\left(\frac{\vec{V}_{1(cyc)}}{\vec{I}_{1(cyc)}}\right)$, where $\vec{V}_{1(cyc)}$ and $\vec{I}_{1(cyc)}$ are the positive sequence voltage and resistance after a short settling period somewhere between 1-8 power cycles,

or $R_P = \text{minimum}[R]$ which is the minimum resistance during the start-up, also

requiring some time to be calculated (Zocholl, 2010, p. 5). This causes a short delay in the thermal level calculations. However, this does not affect the thermal level calculations in a too harmful way, since as the slip will remain at the value 1 a bit longer, the thermal level value will therefore also be slightly higher. This makes the calculations a bit less accurate, however slightly overestimating the thermal level meaning that the rotor is at least not insufficiently protected.

Another way of calculating the stator resistance is proposed in the paper written by Whatley et al., where the possible lack of motor information is taken into consideration by estimating some parameters. In the paper the stator resistance is calculated as $R_{SI} = 3 * R_N$ (Whatley et al., 2008, p. 211).

Lastly, in the book AC motor protection, Zocholl introduces a third also quite a simple way to calculate the stator resistance $R_{SI} = \frac{R_N}{5}$ (Zocholl, 2003, p9). The values of the second and the third way should differ from each other quite a lot, which makes the significance of the initial stator resistance questionable.

4.3 Rotor thermal model

The literature and the standard IEC 60255-149 provide a thermal circuit model based on which both the rotor and stator thermal model can be modeled from. Figure 10 represents the standard IEC 60255-149 version of the thermal circuit as well as the electrical circuit model equivalent. The current source (I) is regarded equivalent to the power supplied to the equipment in the thermal process ($I^2 r$) and the temperature in the thermal process ($\theta(t)$) is equivalent to the voltage ($V(t)$) across the capacitor in the RC circuit (IEC 60255-149, 2013).

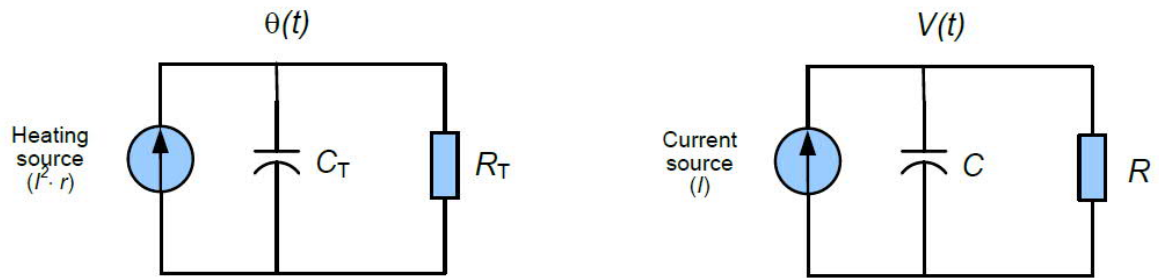


Figure 10 Motor presented as a first-order thermal system and an electrical RC circuit (IEC 60255-149, 2013).

In his written work, Zocholl has modified the first-order thermal system to represent the rotor thermal system (Figure 11) and the stator thermal system (Figure 12).

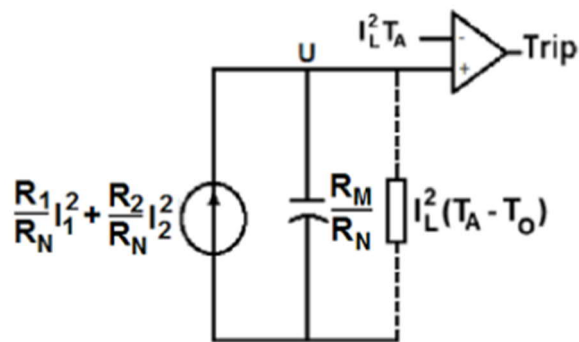


Figure 11 Rotor thermal circuit model (Zocholl, 2007)

Equations for the rotor thermal level can be formed from the rotor thermal system model, resulting in two equations which are used depending on the measured current I (Zocholl, 2007):

$$U_n = \left(\frac{R_1}{R_N} I_1^2 + \frac{R_2}{R_N} I_2^2 \right) \frac{\Delta t}{C_{Th}} + U_{n-1}, \quad \text{when } I > 2.5 \text{ (pu)} \quad (14a)$$

$$U_n = \left(\frac{R_1}{R_N} I_1^2 + \frac{R_2}{R_N} I_2^2 \right) \frac{\Delta t}{C_{Th}} + \left(1 - \frac{\Delta t}{R_{Th} C_{Th}} \right) U_{n-1}, \quad \text{when } I < 2.5 \text{ (pu)} \quad (14b)$$

where U_n thermal level at sample n ,

R_1 is the rotor positive sequence resistance,
 R_N is the rotor nominal speed resistance,
 I_1 is the motor positive sequence current,
 R_2 is the rotor negative sequence resistance,
 I_2 is the negative sequence current,
 Δt is the time step between the samples,
 C_{Th} is the thermal capacitance,
 R_{Th} is the thermal resistance and
 U_{n-1} is thermal level at sample $n - 1$

The thermal level values obtained by equation 14a and 14b are compared to the rotor trip level $I_L^2 * T_A$

In equations 14a and 14b, the thermal capacitance C_{Th} can be considered to be an adiabatic time constant, meaning that no energy is transferred between the system and the environment, and it is calculated as:

$$C_{Th} = \frac{R_M}{R_N} \quad (15)$$

The thermal time constant for when current is below 2.5 per unit, and the process is not anymore considered to be adiabatic, is $R_{Th} * C_{Th}$, where the thermal resistance R_{Th} is calculated as:

$$R_{Th} = I_L(T_A - T_O), \quad (16)$$

where I_L is the locked rotor current in per unit of full load current,
 T_A is the cold motor stall time limit and
 T_O is the hot motor stall time limit.

4.4 Stator thermal model

The thermal model of the stator is calculated alongside the rotor thermal model and is slightly simpler as it does not require slip estimation. Figure 12 represents the stator thermal circuit model from which the stator thermal level equation is formed from.

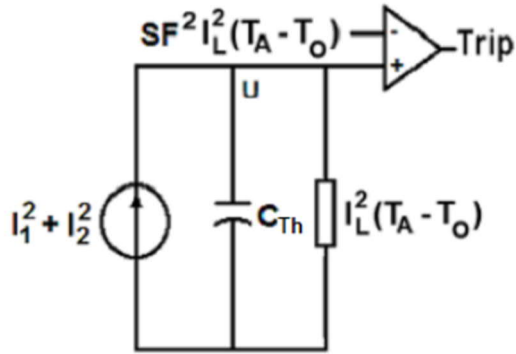


Figure 12 Stator thermal circuit model (Zocholl, 2007).

The stator thermal model is calculated as such (Zocholl, 2007):

$$U_n = (I_1^2 + I_2^2) * R_{Th} \frac{\Delta t}{C_{Th}} + \left(1 - \frac{\Delta t}{R_{Th} C_{Th}}\right) U_{n-1}, \quad (17)$$

where U_n thermal level at time n ,
 I_1 is the positive sequence current,
 I_2 is the negative sequence current,
 R_{Th} is the thermal resistance,
 Δt is the time delta,
 C_{Th} is the thermal capacitance and
 U_{n-1} is thermal level at time $n - 1$

The thermal level values are compared to the stator trip level, and if the level is exceeded the relay will trip.

While in stator thermal model the thermal resistance R_{Th} is calculated similarly as in the rotor thermal model, the thermal capacitance C_{Th} is calculated differently:

$$C_{Th} = \frac{\tau}{R_{Th}}, \quad (18)$$

where τ is a thermal time constant and R_{Th} is the thermal resistance.

The thermal time constant τ is calculated as such:

$$\tau = \frac{(T_A - T_O)/2}{\ln\left(\frac{I_L^2 - I_{prior}^2}{I_L^2 - SF^2}\right)}, \quad (19)$$

where T_A is the cold motor stall time limit,
 T_O is the hot motor stall time limit,
 I_L is the locked rotor current,
 I_{prior} is the prior load current and
 SF is the service factor.

4.5 Current ABB thermal protection

The literature, regarding slip-dependent thermal models, has separate thermal models for rotor and stator, in which slip-dependent rotor resistance is used to distinguish the rotor thermal model (Zocholl, 2007). ABB motor thermal protection function has a combined model which covers both stator and rotor. The model calculates separate thermal level values for the stator and for the hotspots when an overload situation occurs. The rotor is acknowledged as a hotspot, which heats up more in the start-up compared to the stator.

The current ABB motor thermal protection function is formulated as follows:

$$\theta_B = \left(\left(\frac{I}{k \cdot I_r} \right)^2 + K_2 * \left(\frac{I_2}{k \cdot I_r} \right)^2 \right) * \left(1 - e^{-\frac{t}{\tau}} \right) * p\% \quad (20)$$

$$\theta_A = \left(\left(\frac{I}{k \cdot I_r} \right)^2 + K_2 * \left(\frac{I_2}{k \cdot I_r} \right)^2 \right) * \left(1 - e^{-\frac{t}{\tau}} \right) * 100\% \quad (21)$$

where θ_B is the thermal level when no overload is present,
 θ_A is the thermal level when overload is present,
 I is the TRMS value of the measured max of phase currents,
 I_r is the set Current reference, FLC or internal FLC,
 I_2 is the measured negative sequence current,
 k is the set value of Overload factor,
 K_2 is the set value of Negative sequence factor,
 p is the set value of Weighting factor and
 τ is the time constant.

The TRMS refers to true root mean square, which is a way to calculate the direct current equivalent value. FLC is an abbreviation of full load current. The Weighting factor is used to determine the ratio of the thermal increase of the two curves.

The Negative sequence factor is used to take into account the excessive heating of the rotor. The factor is the ratio of the rotor negative and positive sequence resistances, which can be approximated to be 5.

Equations 20 & 21 are used to model the thermal level when the motor is running. Equation 21 is used whenever the measured stator current exceeds a specified overload limit. This occur mostly during the start-up. Equation 20 is used otherwise. The time constant τ is changed according to the stator current.

After an overload situation, as long as θ_A is higher than θ_B , the θ_A value is decreased with a constant speed until it reaches the same value as θ_B . Even though this is a

simplification, it aims to model how the hotspot temperatures stabilize and decrease towards the motor body temperature.

5 Development of the thermal protection algorithm

This chapter is hidden as authenticated and protected information by ABB.

5.1 Slip dependent rotor model

5.2 Function proposal

5.3 Stator model with RTD

6 Evaluation of developed algorithms with a simulated motor start

A goal of the thesis is to develop a new thermal protection algorithm, and an important part of the development is to test the algorithm. The testing will be done with simulated data. This should provide verification and valuable insight if the algorithm works as intended.

The simulated data is used to prove that the algorithm successfully calculates the motor slip. Additionally, the algorithm will be tested in two unwanted conditions: current unbalance and measuring current transformer saturation.

6.1 Simulation model with PSCAD™

A power system simulation tool, PSCAD™, is used to create a model of a power network and a squirrel cage induction motor, and to simulate data. This model can then be used to generate currents and voltages similarly as in a real-life power system. Additionally, the model outputs the speed of the rotor which can be used to compare to the slip estimated from the simulated currents and voltages.

Unfortunately, the model cannot output the thermal level of the stator or the rotor, so the testing target is mainly the slip estimation. However, it is still valuable to test that the calculated thermal level values are approximately correct.

The model itself consists of one squirrel cage induction motor, a voltage source, three transformers and a passive load connected to the grid (Figure 14). Also, a breaker and a timer were set to time when an electrical load would be applied to the motor and when the motor would be energized. This time was set to 0.5 seconds, which is the starting time of the motor in the simulated data.

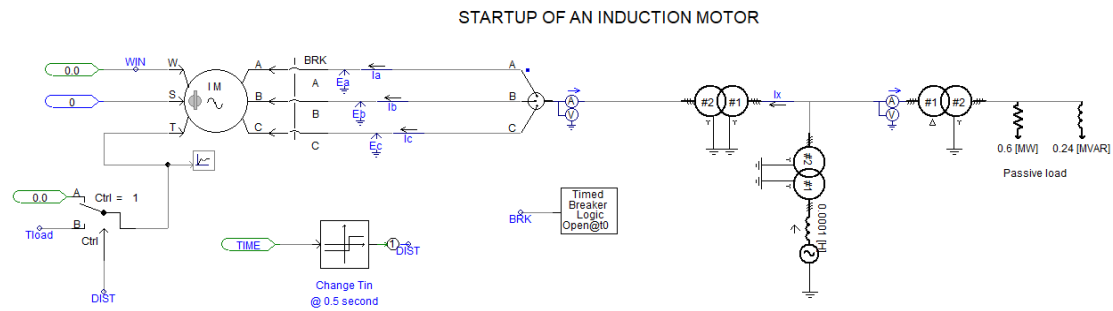


Figure 13 Power system model with a squirrel cage induction motor.

The motor information that the simulation model uses is from an actual ABB motor. Figure 15 shows an information input window, in which the basic information about the motor is configured. The set voltage is the rated RMS (root-mean-square) phase voltage and the set current is the rated RMS phase current. The base angular frequency describes the grid frequency, which is 50 Hz.

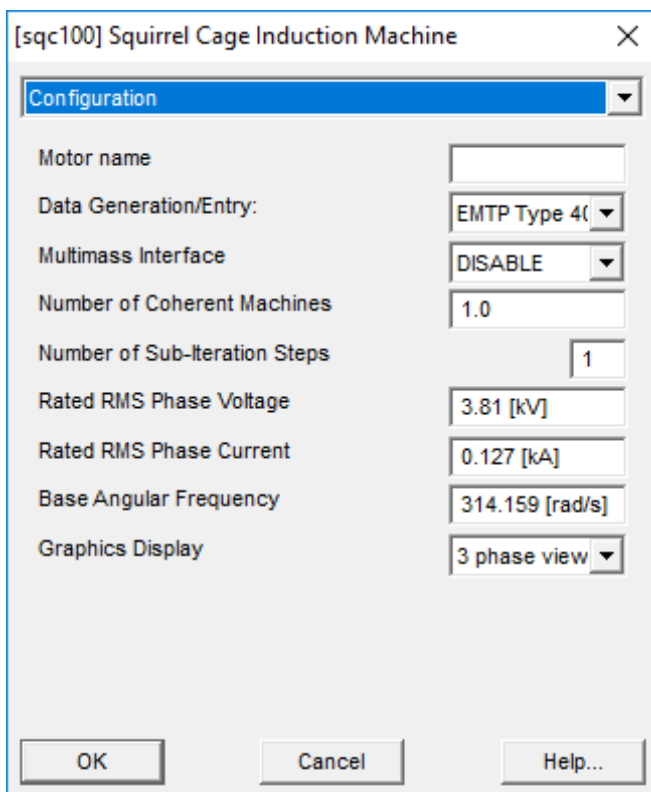


Figure 14 PSCAD motor information configuration window.

The simulation tool allows the user to input the motor information in different ways, varying from only configuring the motor based on the horsepower to configuring the motor based on multiple inputs describing the motor. The more input parameters the model has the more accurate it becomes. Since, a motor data sheet was available, the model was able to be configured precisely.

The simulation tool motor was configured with the EMTP (Electromagnetic Transients Program) Type 40 format Figure 16.

The image shows a software window titled "[sqc100] Squirrel Cage Induction Machine" with a close button (X) in the top right corner. A dropdown menu at the top is set to "EMTP Type 40 format". Below this, there are several input fields for motor parameters:

Design Ratio	1 [pu]
Power factor at rated load	0.89 [pu]
Efficiency at rated load	0.968 [pu]
Slip at full load	0.005 [pu]
Starting current at full volts	5.9 [pu]
Starting Torque at full volt / Full load torque	0.58 [pu]
Maximum Torque / Full load torque	2.3 [pu]
Number of poles	2
Polar moment of Inertia (J)	40.2
Units of the inertia	kg*m^2
Mechanical Damping	0.008 [pu]

At the bottom of the window, there are three buttons: "OK", "Cancel", and "Help..."

Figure 15 The EMTP Type 40 format configuration window.

Most of the inputs are in per unit, which presents the value in a ratio relative to a base value. For example, the starting current is 5.9 times the value of the rated current. The per unit system is used to allow more meaningful comparison between different quantities, since they are scaled similarly.

6.2 Verifying slip and thermal calculation with PSCAD™ data

Since the rotor thermal model is based on slip, it is essential to confirm that the slip estimate calculation is accurate enough. The calculation does not have to be exact, but it should not differ by a large margin, so that the thermal level calculations would remain valid. It is difficult to define a precise limit to how much the calculations can be allowed to differ, but if the thermal level calculated with the estimated slip is much smaller than with the PSCAD™ one, the thermal protection is insufficient.

Even though a precise configuration was used, the current simulated from the model resulted to be slightly different from what was expected (Figure 17). The high starting current was accurately simulated, but the load current was about half of the value expected.

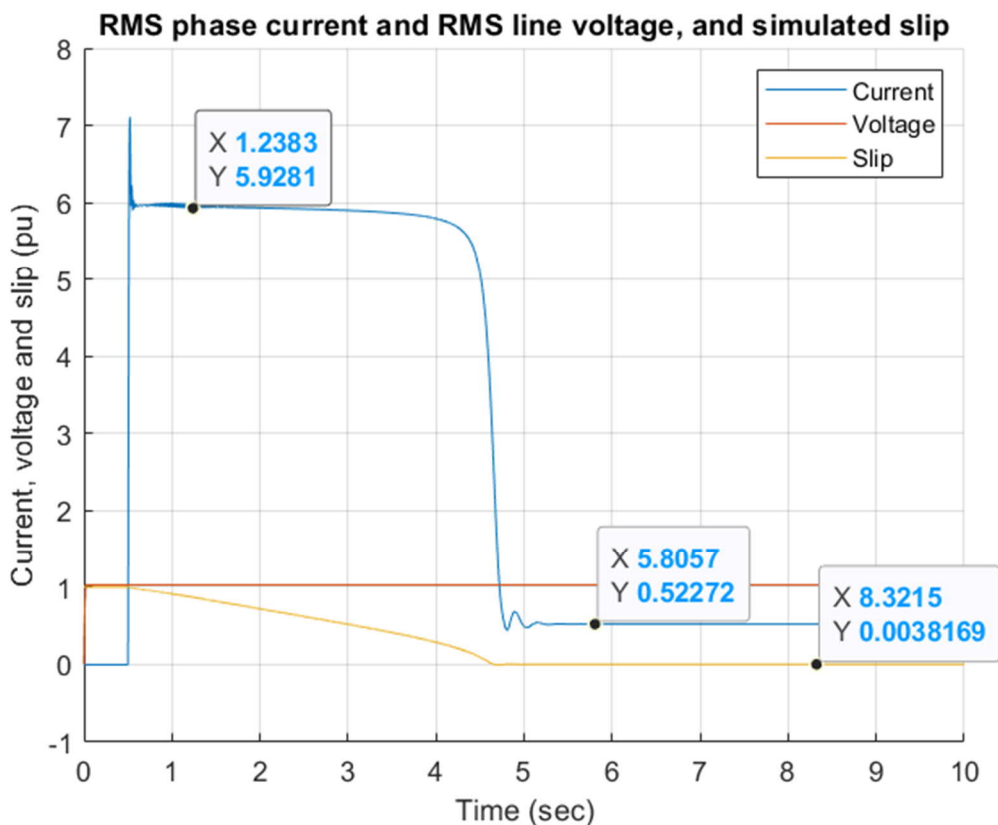


Figure 16 RMS phase currents and RMS line voltages, and simulated slip in per unit, created with the simulation tool.

With the simulated voltage, the values stay the same throughout the simulation period. There is also a possibility that the voltage drops up to about 20 percent after the motor is started, due to the increased load the motor puts on the grid. The voltage drop depends on the supplying power transformer impedance and its apparent power as well as the motors apparent power.

Lastly, the simulated slip has seemed to behave accordingly, however it reaches a slightly lower value than expected. This might also explain why the rated current is lower than expected, as the slip defined to the simulation model was 0.005 per unit. It is possible that the mathematical model behind the simulation tool fail to produce authentic data. However, the data seems to be accurate during the start, where the most change to the slip occurs.

The essential use of the simulated data was to compare the estimated slip to the simulated one. The estimated slip is calculated from the simulated currents and voltages, which can also be assumed to have been used in the simulation tool slip calculations. The premise was that the results should be similar, but some difference could occur due to the fact that the simulation tool might calculate the slip in a more complex fashion. Whereas the slip estimation is intended to be used in protection functions, so some simplifications can be assumed. Figure 18 shows two plots of a start-up situation, the upper presenting the comparison between estimated slip calculated in two different ways, and simulated slip. The lower plot contains the same curves, but the view is zoomed in order to illustrate the values which the slip stabilizes.

The two slip estimations are calculated with different ways to define the initial stator resistance from the motor positive sequence resistance. In one the stator resistance is calculated at a predetermined point, the 6th power cycle, during the start-up, and in the other the smallest value calculated during the first 0.5 seconds after the motor was energized is used.

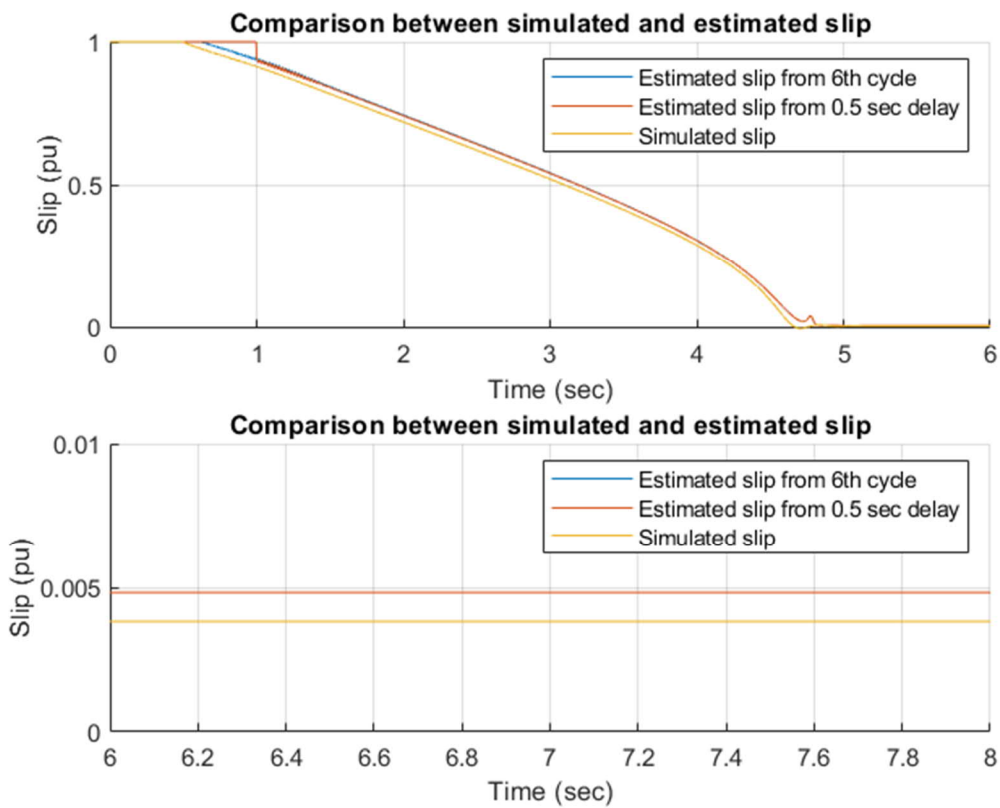


Figure 17 Comparison between two slip estimations and one simulated slip.

Looking at the upper plot, the differences between the slips are marginal except for right after the start where both estimated slips differ from the simulated one. These differences are caused by the time it takes to define the stator resistance, these times being six power cycles i.e. 0.12 seconds and 0.5 seconds. Although, unnoticeable from the upper plot, there is also a slight difference in the rated slips, which is depicted in the lower plot. However, this difference is diminishing and the end result of the slip estimation with simulated data is quite satisfactory. The diminishing difference is also present between the two estimated slips, which result in the same nominal value, therefore only the other is showing in the plot.

The rotor resistance factor is linearly derived from slip. Therefore, the rotor resistance factor graph is similar to slips (Figure 19). This factor is used in the thermal level calculations to weigh in the heating effect of the rotor during different speeds.

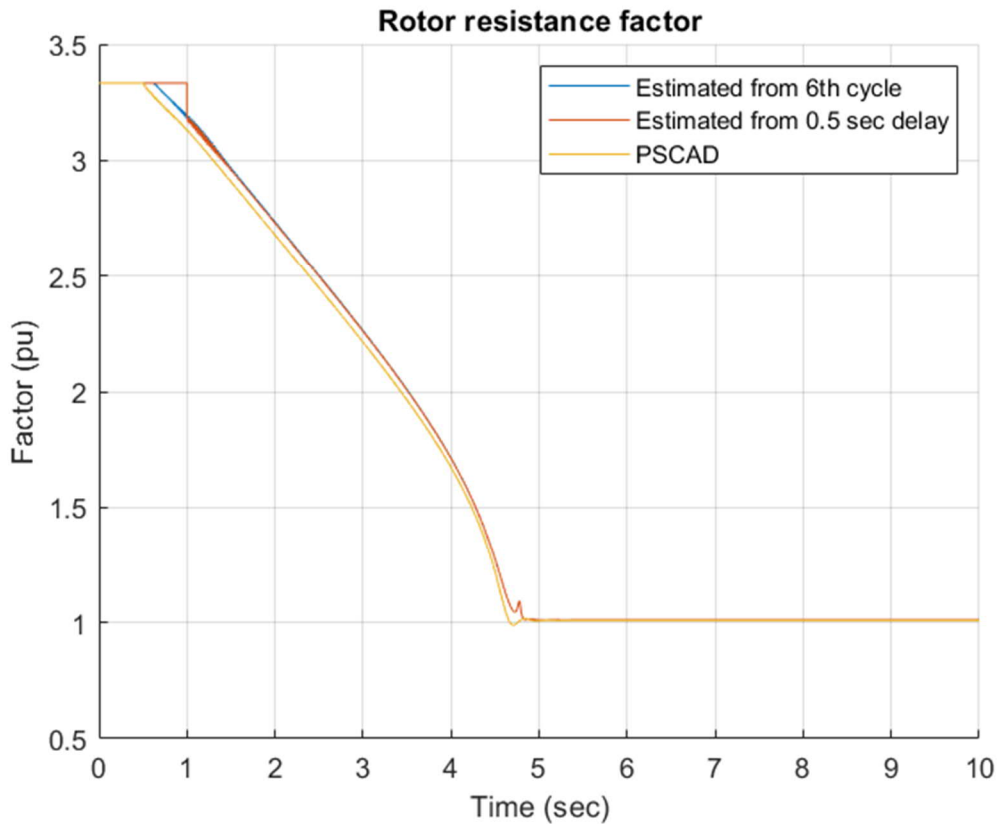


Figure 18 Rotor resistance factor comparison.

The positive sequence rotor resistance obtains the value one at nominal speed, and as mentioned in the Chapter 4, the value is roughly three times larger when the rotor is not moving. And although not depicted, the negative sequence resistance minimal value is two, whereas the highest value can increase up to five.

As could be deduced from the slip and rotor resistance factor comparisons, also the thermal level calculations yielded very comparable results. Figure 20 contains two plots, the upper presenting the thermal levels calculated with the two estimated and one simulated slip, and the lower illustrates the absolute differences between the thermal levels calculated from the estimated slips and the simulated slip.

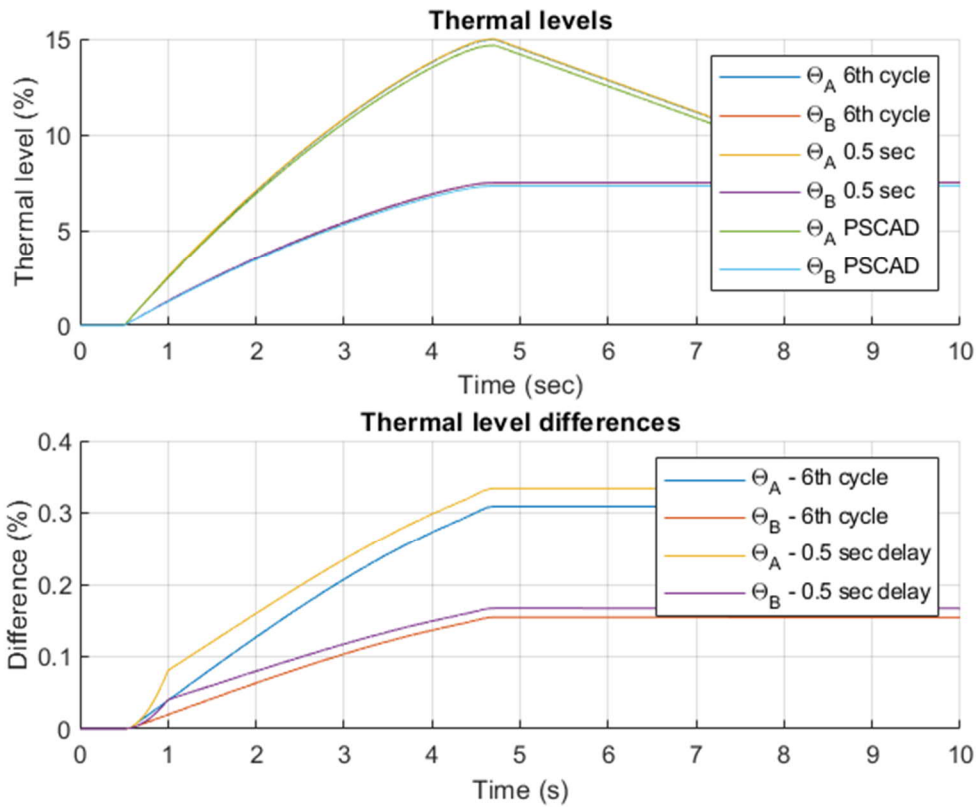


Figure 19 Rotor thermal levels and thermal level absolute differences. θ_A is the thermal level for overload situation and θ_B is for nominal run.

There is only a miniscule difference between the estimate-based and simulation-based thermal levels as they differ only by a bit over 0.3 percent at most. From the observations done based on the simulated data, the slip estimation is successful. In retrospect, this result should not be surprising since the simulation tool creates the data based on equations that are probably similar to the ones found in the literature. However, this confirms that the estimation calculations have been done correctly, and the estimation can now be further analyzed.

6.3 Analyzing the function in untypical conditions

As mentioned in chapter 5, it is important from the protection perspective that the function is stable even if affected by untypical conditions such as unbalance or current

transformer saturation. Therefore, the function should be tested under these conditions in order to find out how and how much these conditions affect.

6.3.1 Unbalance analysis

For the unbalance analysis, the simulation model is altered by adding an inductor on one of the phase lines. This creates a small unbalance that can be adjusted with the amount of inductance.

The acceptable amount of unbalance varies, but an example for continuous negative sequence voltage is three percent. The amount of voltage unbalance will appear in current unbalance multiple times larger. This is because, in situation like the motor start-up, the current can be 6 – 10 times larger than voltage unbalance (Pacific Gas and Electric Company, 2009). Most typically, the acceptable amount of continuous current unbalance for induction motors is 8 - 15 percent of the motor rated current. If this amount is surpassed, the relay will trip.

The inductor that was added to the simulation model had the inductance of 1 mH. The unbalance that this created to the voltages and currents is illustrated in Figure 21.

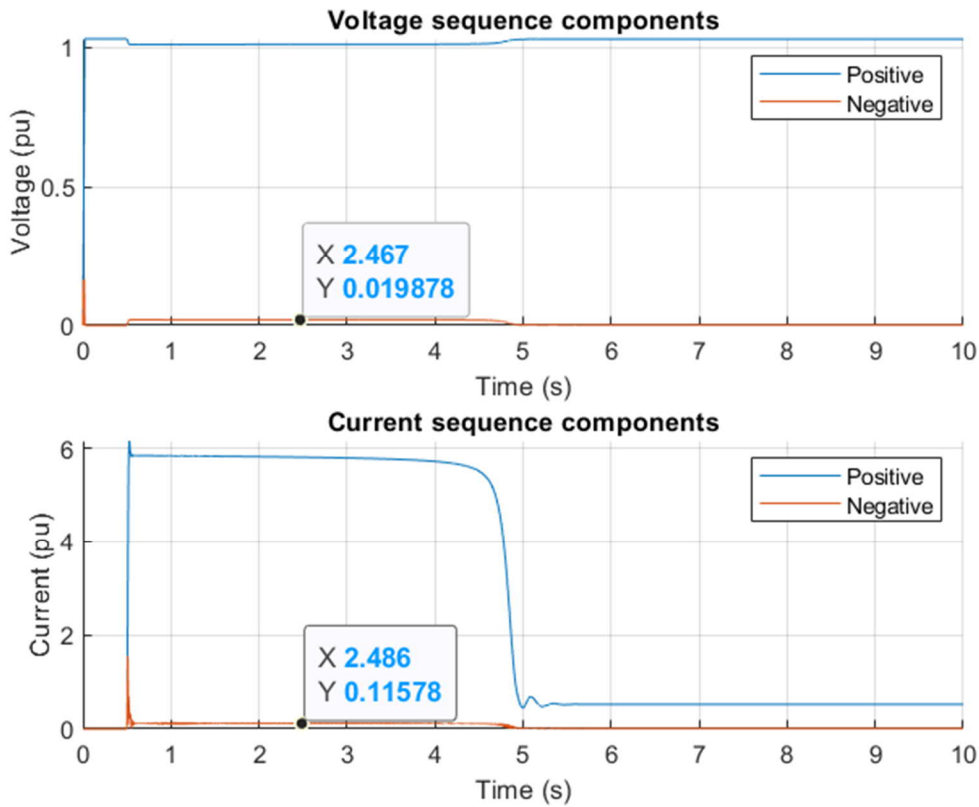


Figure 20 Plots of positive and negative sequence components for voltage and current.

The unbalance is noticeable only during the motor start-up. There the amount of voltage unbalance is about two percent and the amount of current unbalance is about 11.5 percent. As the starting current defined to the simulation model was 5.9 per unit, this result is expected.

The next objective is to investigate whether or not the unbalance has an effect on the slip estimation. As the slip estimation utilizes positive sequence voltage and current, unbalance could be assumed to have some effect. The effect of unbalance on slip estimation is illustrated in Figure 22.

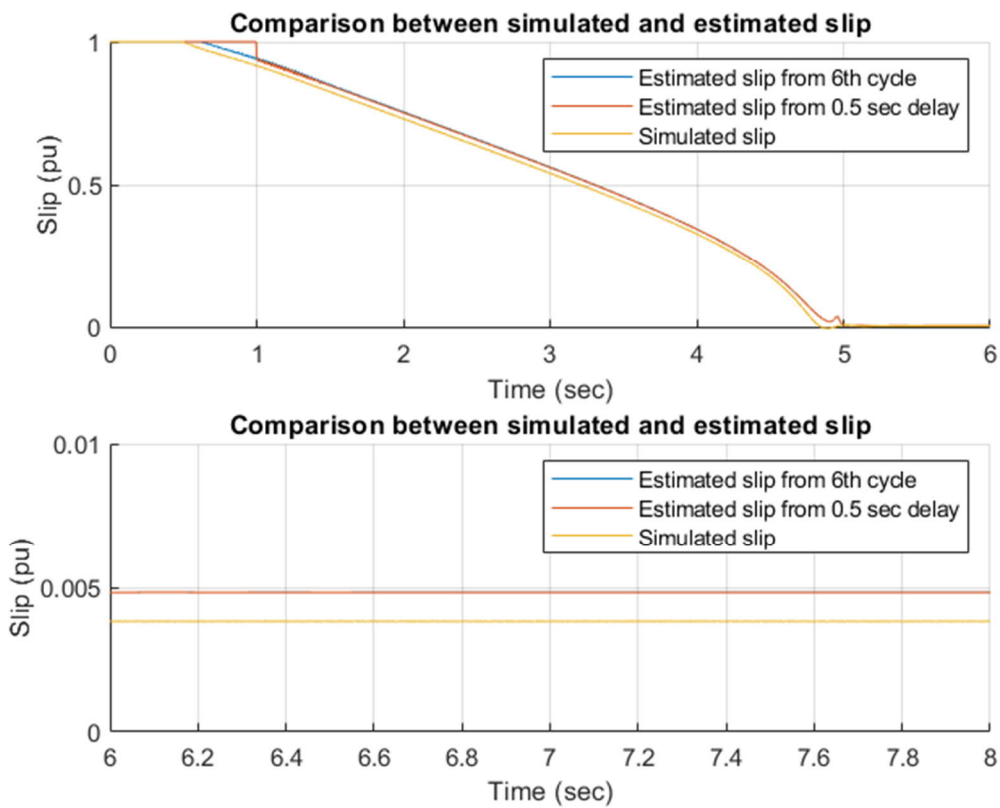


Figure 21 The effect of unbalance on slip estimations.

As the simulation model also takes into account the effect of the unbalance, the comparison is done with the PSCAD™ simulated slip and the two slip estimates, similar to what was done with unaltered PSCAD™ data. The results also look identical, meaning that the slip estimate is not affected by unbalance.

The reasoning behind this could be that since this amount of unbalance clearly in the range of being allowed, even the measured slip is therefore naturally not expected to be particularly affected. And since the slip estimation uses an equation between the voltage and current, and as the unbalance is similarly affecting both, the slip estimate is also unaffected.

This is a good result for the unbalance test as it can be deemed to not affect the slip estimate calculations, and therefore also the thermal level calculations.

6.3.2 CT saturation analysis

Current transformer saturation is a phenomenon that affects the measured current. The current transformer (CT) saturation analysis was implemented using a MATLAB®-based CT simulation tool, made by ABB. The simulation is based on the real-life CT, which was suited for the motor. The CT ratio is 150/5A, the CT accuracy class is 5P, the rated accuracy limit factor is 10, the CT rated burden is 20VA and the secondary winding resistance is 0.2205Ω .

The current that the script takes as an input is altered so, that the output current is affected by a current transformer that has saturated. The degree of saturation is a function of the actual accuracy limit factor F_A . The F_A is proportional to the ratio of the rated CT burden and the actual CT burden. Depending on the current transformer, in motor applications F_A values vary typical between 10 – 30, the lower the value the less accurate the calculation, five being often the smallest acceptable value.

In the test, the F_A value was varied by changing the CT burden [ohm]. By changing this value, the script is able to create the effect of CT saturation to the input current.

The CT burden value was changed so that F_A values varied between 5 – 50. Then the slip estimation calculations are done with each of these affected currents. Lastly, the thermal levels are calculated to investigate if any notable affect is found.

The starting point of the analysis is currents affected by the saturation, since changes in the currents can cause disturbance in the slip estimation. Figure 23 presents the positive sequence currents with different amounts of CT saturation affecting them.

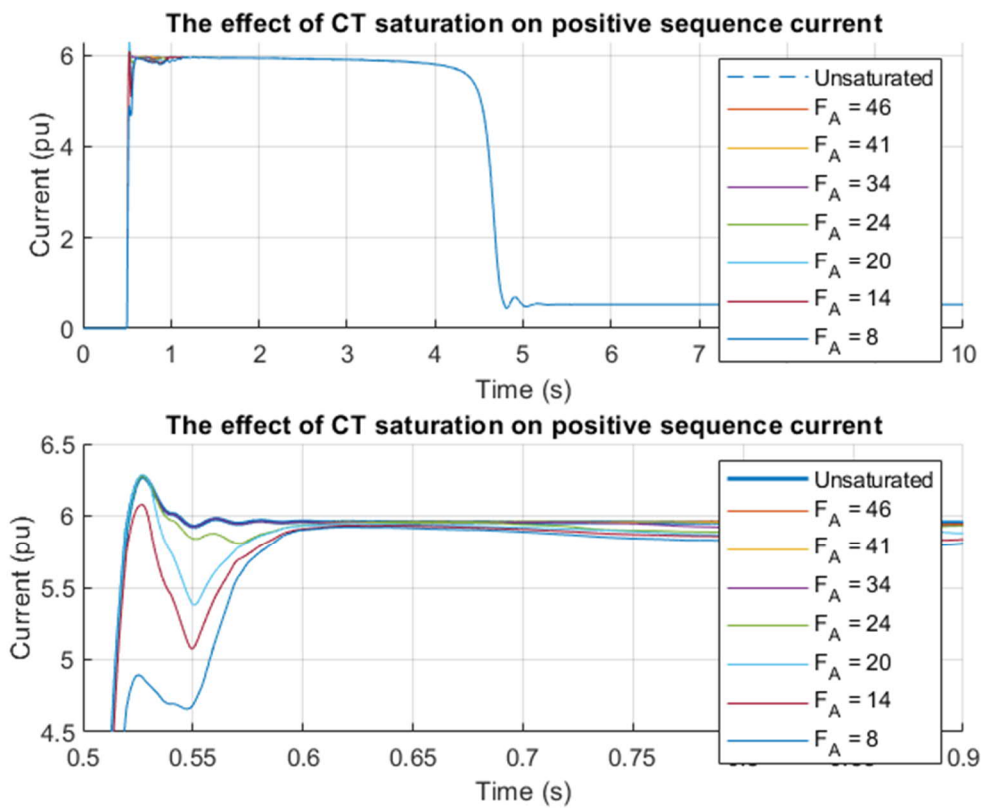


Figure 22 The effect of CT saturation on positive sequence current.

The two plots both show the same positive sequence currents, but the lower is again from a zoomed view. The currents are slightly affected right after the motor start and for a short period after it. The smaller the F_A is the smaller the peak of the current is right after the start. This might affect the slip estimation and defining the initial stator resistance.

In addition to the CT saturation, also the way how the initial stator resistance was defined was used in the analysis. Therefore, two different plots were made for each way to define the initial stator resistance, each plot containing slip estimates calculated with different levels of CT saturation affecting the currents. Figure 24 illustrates the slip estimates calculated with the initial stator resistance defined at the 6th power cycle. And since it takes six power cycles to define the initial stator resistance, the slip estimates will remain at value one for this amount of time.

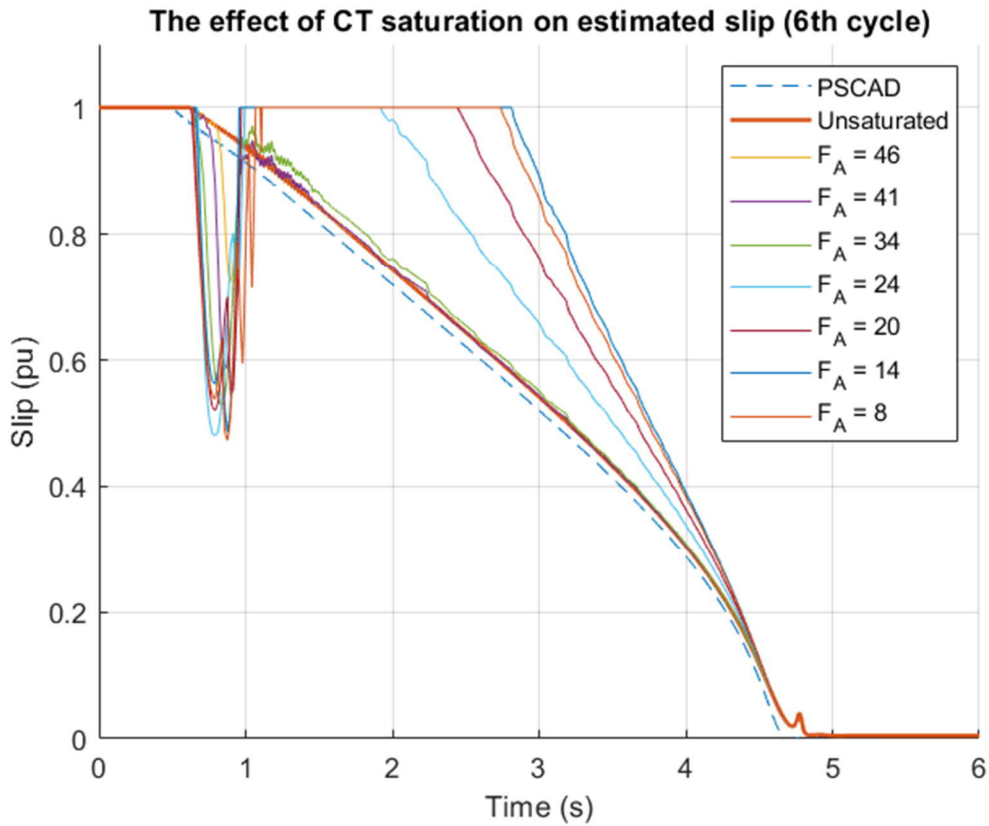


Figure 23 The effect of CT saturation on estimated slip. The initial stator resistance defined at the 6th power cycle.

The slip estimates are quite strongly affected by the CT saturation. The slip estimate curves have a lot of distortion during the six power cycles after the motor start. Also, the affected slip estimates remain close to the value one for relatively long times. Again, the lower the actual accuracy limit factor is, the more distorted the slip estimation becomes. Even though the slip estimates are heavily distorted, they still manage to achieve the rated slip value at the same time as the PSCAD™ slip and the unsaturated slip estimate.

Figure 25 contains the slip estimates calculated with the initial stator resistance defined after a 0.5 second calculation period. During the calculation period the slip estimate value is defined to be one.

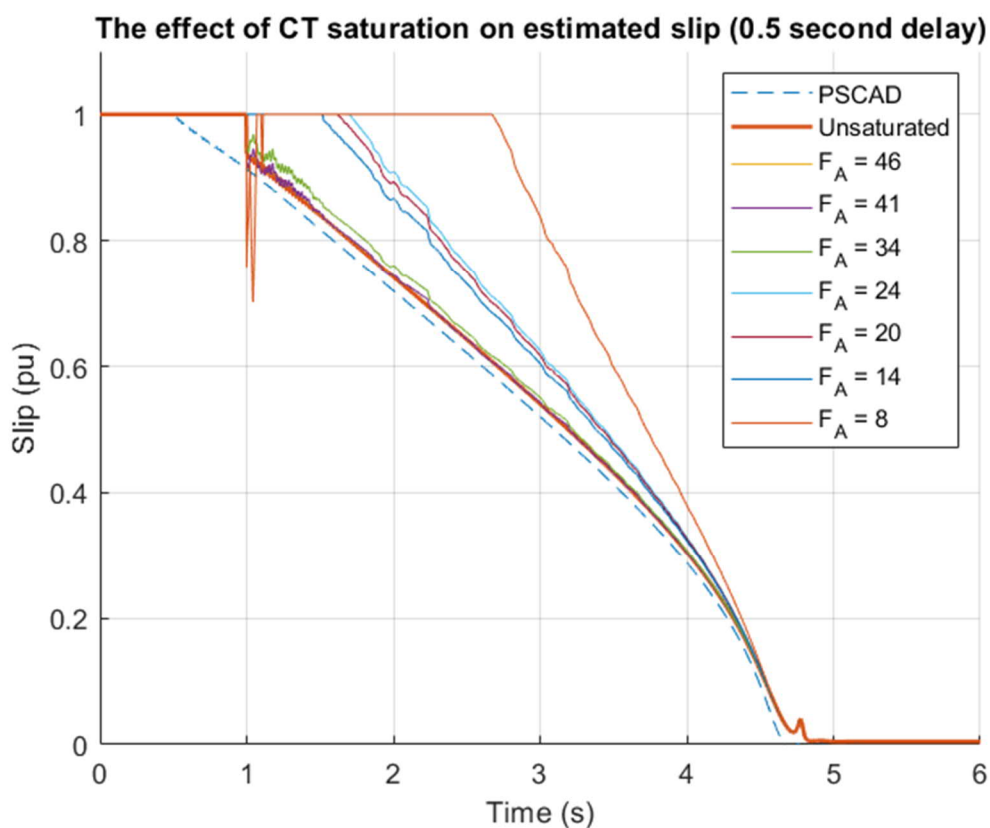


Figure 24 The effect of CT saturation on estimated slip. The initial stator resistance defined after a 0.5 second calculation period.

The slip estimates with F_A values 34, 41 and 46 do not differ from the unsaturated slip estimate. The difference is notable with F_A values 24, 20 and 14, and the difference is quite large with the F_A value 8. These differences appear as the slip estimates remaining at the value one for an extended amount of time. It is fairly certain that this is not the case in a real-life situation, where the rotor would have started rotating. Thereby, the slip estimate seems to become inaccurate if the F_A value is below 34, making it potentially unreliable for locked rotor protection without additional configurations.

Noting that the slip estimates have some larger differences, it is assumed that the thermal levels would differ from the PSCAD™ and unsaturated ones more than previously. The thermal level figures will also be divided between the way the initial stator resistance

is defined. Figure 26 illustrates the thermal levels where the initial stator resistance is defined at the 6th power cycle.

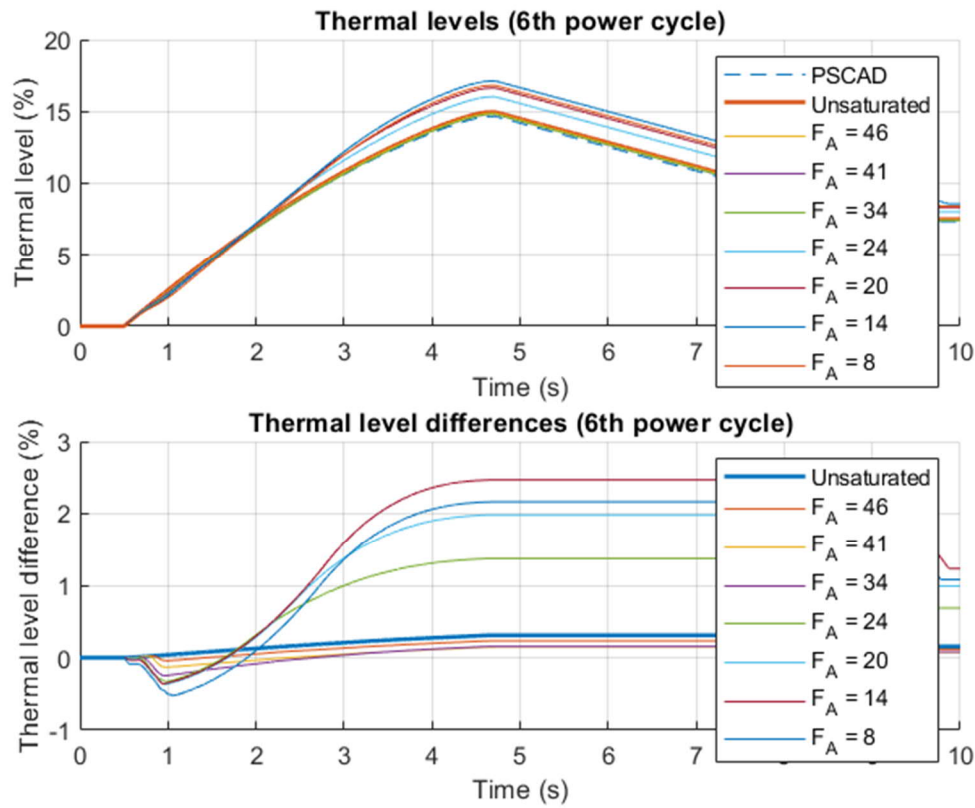


Figure 25 The effect of CT saturation on the thermal levels. The initial stator resistance defined at the 6th power cycle.

The thermal level differences are relatively small, even though the CT saturation impairs the slip estimate accuracy. As the more inaccurate slip estimate values remain close to one, the respective thermal levels should also be increased. However, the distortion in the slip estimate curve start partly balances the increased heating effect, making the thermal level differences remain small.

The slip estimates, where the initial stator resistance was defined during the first 0.5 seconds of the start, showed smaller differences in the slip estimates which also correlate to the thermal levels. Figure 27 illustrates that the differences between the PSCAD

and nearly all the CT saturation affected values are under 1.5 percent with the exception of the curve with the lowest F_A .

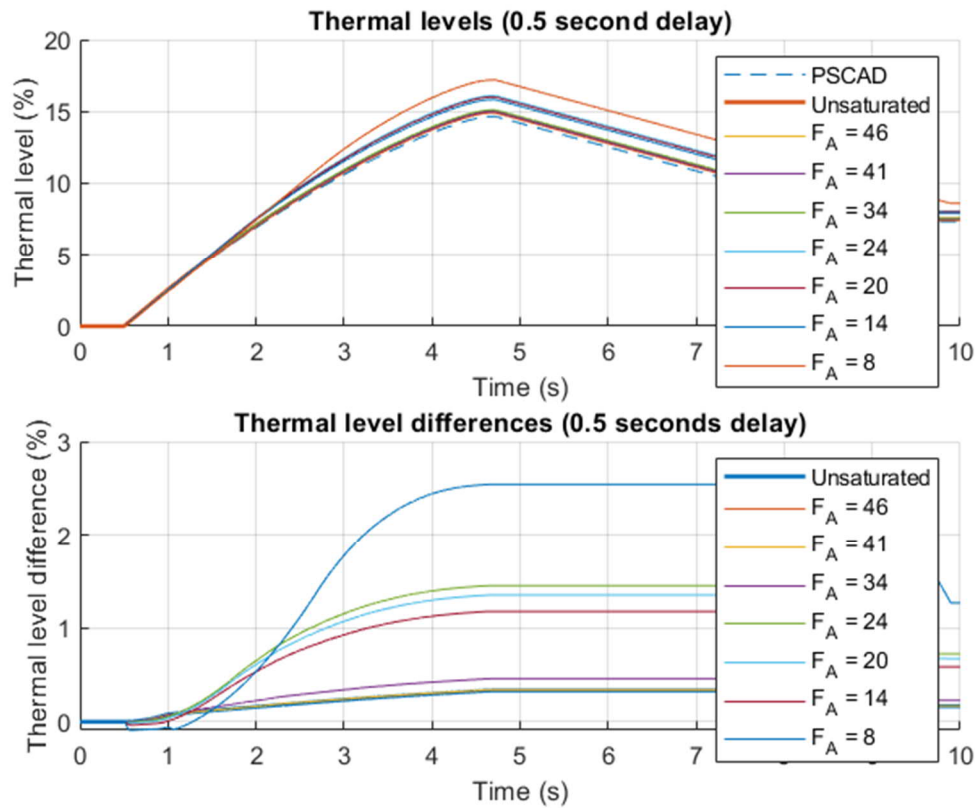


Figure 26 The effect of CT saturation on the thermal levels. The initial stator resistance defined during the first 0.5 seconds of the start.

Although the thermal levels with both of the stator resistance definition methods are quite identical, however both methods have their tradeoffs. The 6th power cycle method allows the calculation to start faster, however it is not as accurate as the 0.5 second delay method. Still, both methods are utilizable to calculate the rotor thermal level, and the 0.5 second delay method being better for locked rotor protection where an accurate slip estimate is required.

7 Field tests in Pietarsaari and testing with actual data

This chapter will discuss about the measurement performed at Alholmens Kraft in Pietarsaari. The measured data will provide means to test and verify the developed algorithm.

7.1 Measurement information

Alholmens Kraft is a power plant located in the western parts of Finland. It is the world's largest biomass-based power plant.

The measurement was performed on a 10-kilovolt, 1000-kilowatt squirrel cage motor. The motor powered a fan the purpose of which was to recirculate the exhaust gases back to the biomass burning chamber in order to reduce the emissions Figure 28.



Figure 27 A fan powered by an induction motor, at Alholmens Kraft.

The energy production process was not active at the time of the measurement. This means that the load is reduced, since the guide vanes were closed there was no pressure from the burning chamber resisting the airflow. This implies that the load current is closer to a no-load current.

The motor was started three times in succession. The first start was from ambient temperature and the other two from operating temperature, totaling one cold and two hot starts. There were no functional abnormalities, although as the motor had not been started for a while the fan had gathered a lot of dust onto it. As the motor was first started the dust blew in the air, slightly impairing the visibility.

The measurements consisted of phase current and phase voltage measurement, and the speed measurement. The current and voltage measurement was performed in the power plant electrical room, and the speed measurement was done from the motor axle with a tachometer (Figure 29). The tachometer was set to record the rotor rotations as pulses, each full rotation equaling one pulse. The first measurement caused some concern due to the dust cloud possibly preventing the tachometer from receiving pulses.



Figure 28 Tachometer measuring the rotational speed from the motor axle.

7.2 Verifying slip estimation with measured data

Similarly, to what was done in Chapter 6, the slip estimate was compared to the measured slip to verify that the calculations give a reasonable result. Again, there might be some differences between the estimated and the measured slip, which might be caused by either simplifications in the calculations or measurement related errors or noise. The measurement current transformer might also have an impact on the estimated slips.

Firstly, the measured data was be analyzed to check if there are any abnormalities. Figure 30 illustrates the measured currents, voltages and slip for each motor start. The tachometer pulses were first converted to speed which was ultimately converted to slip.

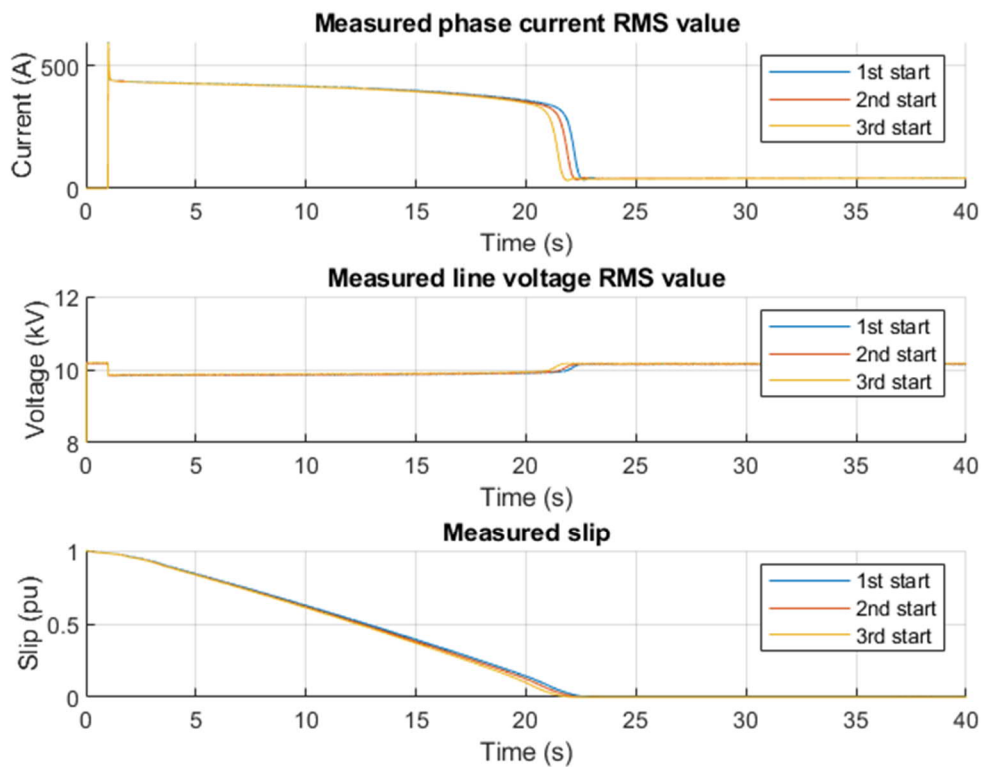


Figure 29 Illustration of the measured currents, voltages and calculated slip from the tachometer measurement.

The measured slips were also filtered using a moving average filter in order to smooth the edges that the conversion from the pulses added.

The measured currents are similar to what was seen in the PSCAD™ simulated data. Although the starting current is same as the motor data sheet, the load current was roughly half of the rated value. This was expected since the motor was expected to run at a lower load.

The measured voltages dropped slightly when the motor was energized, which is expected for motor start-ups. All in all, the measured data seems reasonable and no errors were found that would affect the analysis.

Now that the measurements are deemed to be sufficiently accurate, the slip estimation can follow. As three measurements were done, there will also be three different comparisons between the estimated and measured slip.

Figure 31 illustrates the comparison between the estimated slips and the first measured one. A lot of distortion is occurring with the slip estimate where the initial stator resistance is defined at the 6th power cycle, whereas the one defined during the first 0.5 seconds only has a small distortion right after the motor start. The 0.5 second method also slightly differs from the measured slip during the entire duration of the start-up, however both estimated slips manage to settle to the nominal slip values at the same time as the measured slip.

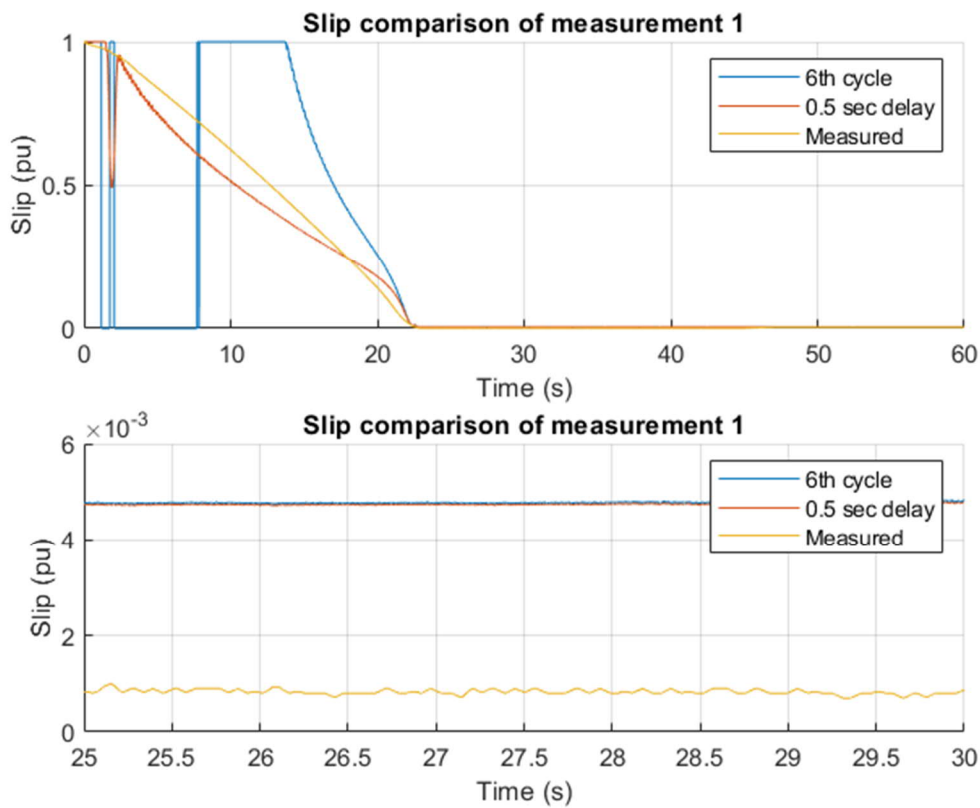


Figure 30 Slip comparison of the first measurement. The lower plot is a zoomed in view from the upper.

The lower plot shows the nominal slip values more closely. Both estimated slips end up close to the value 0.005, whereas the measured slip ends up to 0.001. This is lower than the motors rated speed suggests, which would indicate the slip to be 0.004 at nominal load. However, the motor was not run at nominal load, which results to the motor reaching lower slip values.

The second measurement showed better results for the 6th power cycle method. In Figure 32 the estimated slip curves were quite identical. This implies that the initial stator resistance values are close to each other. However, both estimated slips differ from the measured one during the start-up.

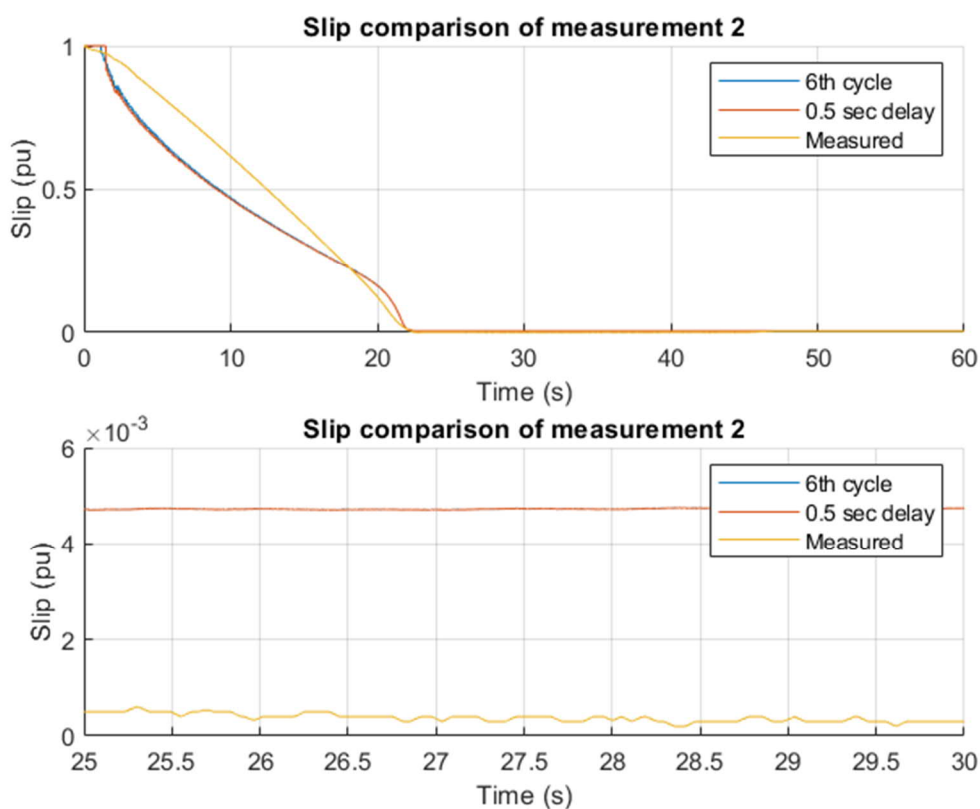


Figure 31 Slip comparison of the second measurement.

The nominal slip values are similar to the first measurement, where the estimated slips resulted in a higher value compared to the measured one.

The third measurement resulted close to similar results as the second. In the upper plot in Figure 33 the same phenomenon can be seen with the estimated slips as in the second measurement. However, right after the start-up there is a steep drop in the estimated slip values, similar to the first measurement. This drop also resembles the behavior illustrated with the CT saturation analysis. Even though the drop is brief, it would still cause some inaccuracies if used in a locked rotor protection.

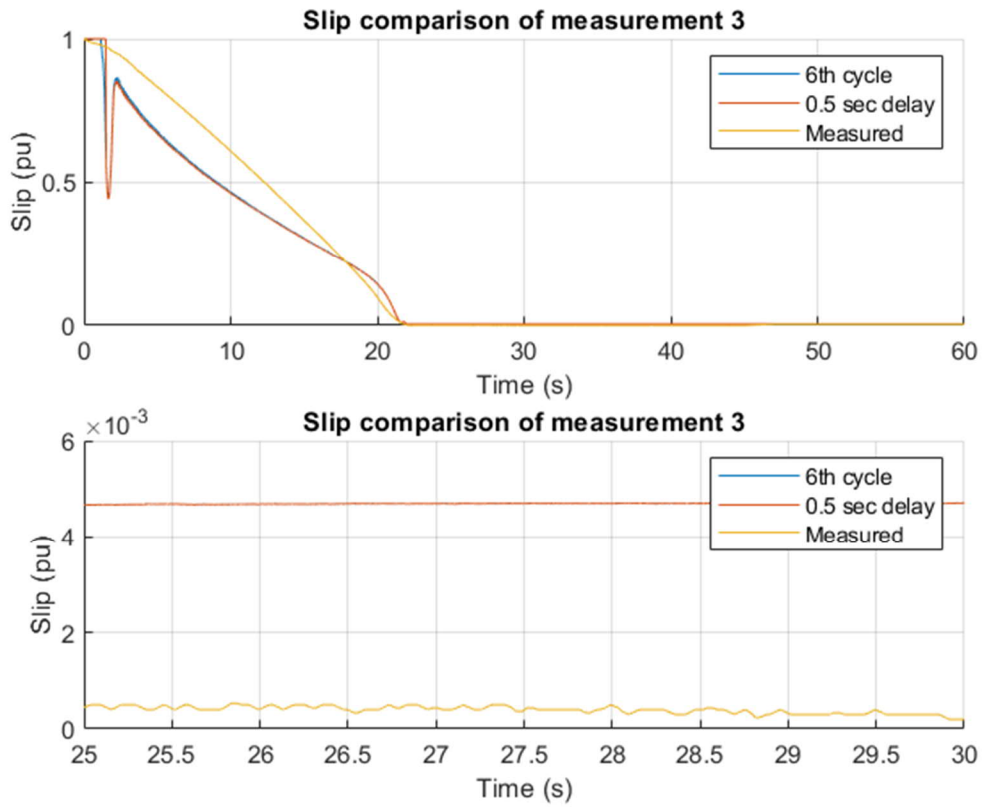


Figure 32 Slip comparison of the third measurement.

The measurements one and three had some fluctuations in the slip estimates, especially right after the motor start. The possible cause to this fluctuation can be found from the calculated motor positive sequence resistances. Figure 34 represents the calculated motor positive sequence resistances from all three measurements.

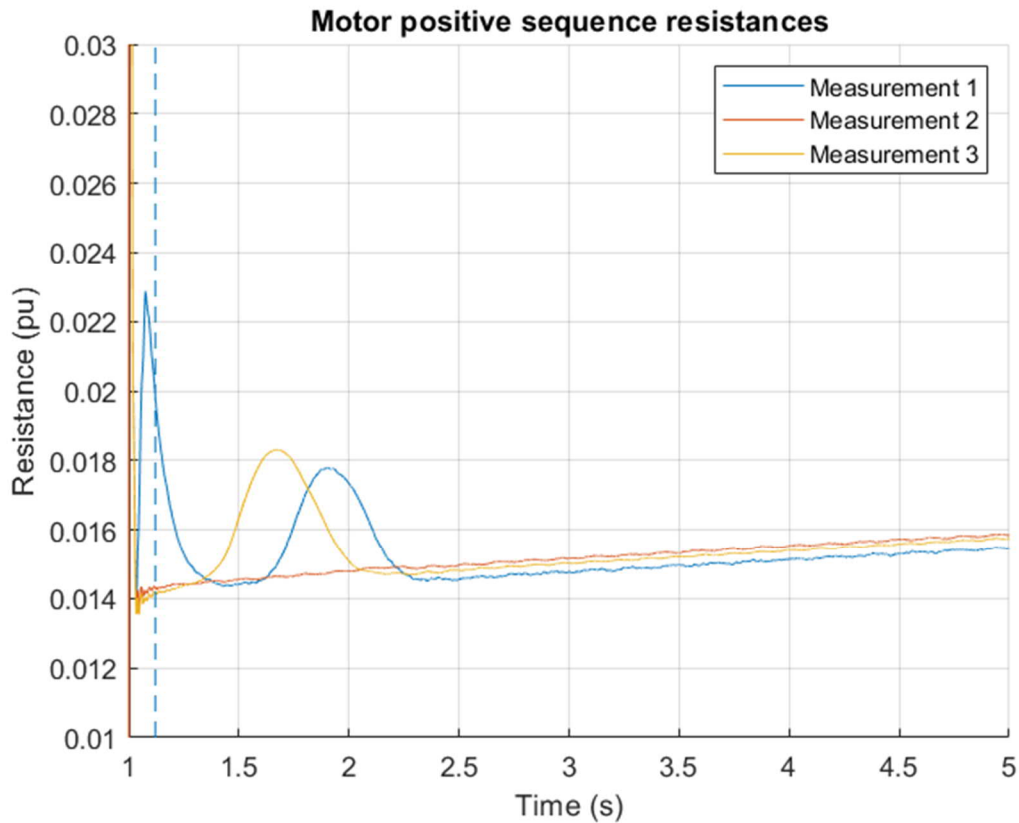


Figure 33 The calculated motor positive sequence resistances for each measurement. The 6th cycle marked with a dashed line.

There is some fluctuation in the resistance calculations of the first and the third measurement starting from 1.5 seconds to 2.3 seconds. Additionally, measurement one has a sharp peak, which happens to occur close to the 6th power cycle, explaining the harsh disturbance that was illustrated in Figure 27. As this fluctuation appears right after the motor start, it could be presumed to be due to the CT saturating.

Although the estimated slips were not identical to the measured ones, the differences, at least for the 0.5 second method, were quite small, making them potentially utilizable for locked rotor protection if configured in a way that takes into account the presumed partial CT saturation.

The next step was to investigate if the estimates are utilizable for thermal level calculations. Comparisons are made between the thermal levels calculated from the measured slip and the thermal levels calculated from the estimated slips. The comparisons are done similarly as in Chapter 6.

Starting with the first measurement, seen in Figure 35, the thermal levels differ by a lot due to the fluctuation caused by the challenging definition of the initial stator resistance.

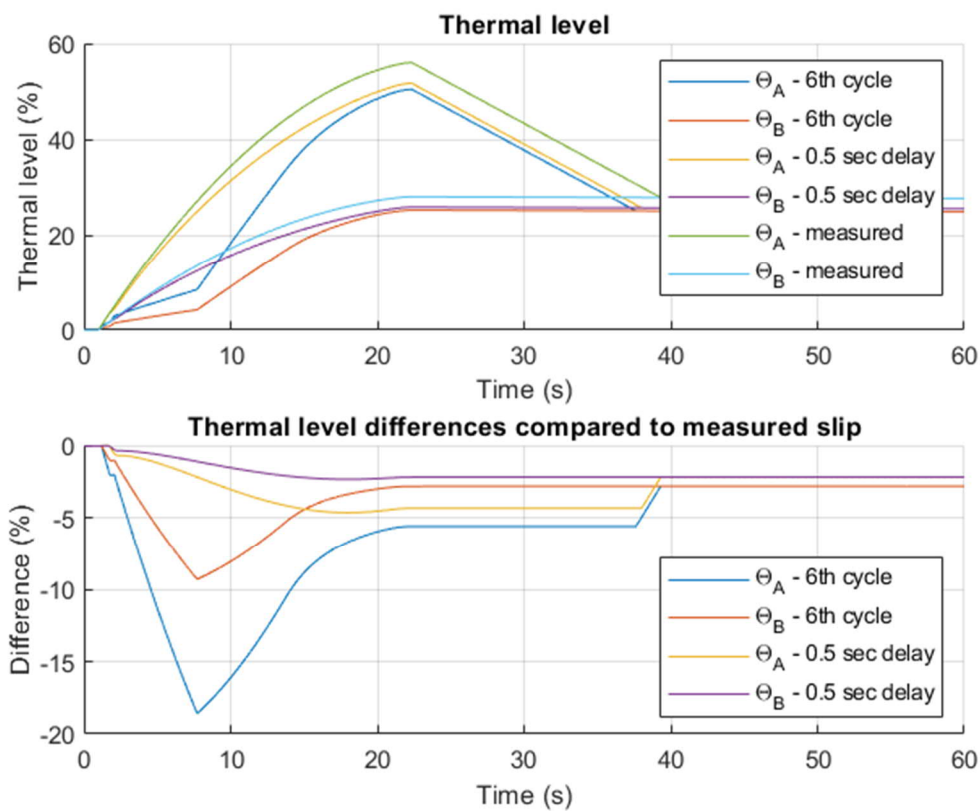


Figure 34 Comparison of the thermal levels of the first measurement.

The thermal levels reach roughly 50 percent. As the start took 21 seconds, and the maximum stall time is defined to be 30 seconds, the expected value with the defined starting current, 6.2 per unit, should be 70 percent, also assuming the rotor is locked. However, as the rotor was not locked and the skin effect gradually faded over the course of the start, the thermal level calculations seem valid.

There are differences between the thermal level based on the measured slip and the thermal levels based on the estimated slips. The thermal level based on the slip estimate calculated with the 6th power cycle method differs substantially, and the thermal levels are also smaller. This is would risk the protected motor to become overheated, while the thermal levels show otherwise. The thermal levels based on the 0.5 second method have smaller difference, being about 5 percent smaller than thermal levels based on the measured slip. This difference, while again being on the bad side, is small enough to be utilized.

The second measurement shows better results for both estimated slip methods (Figure 36).

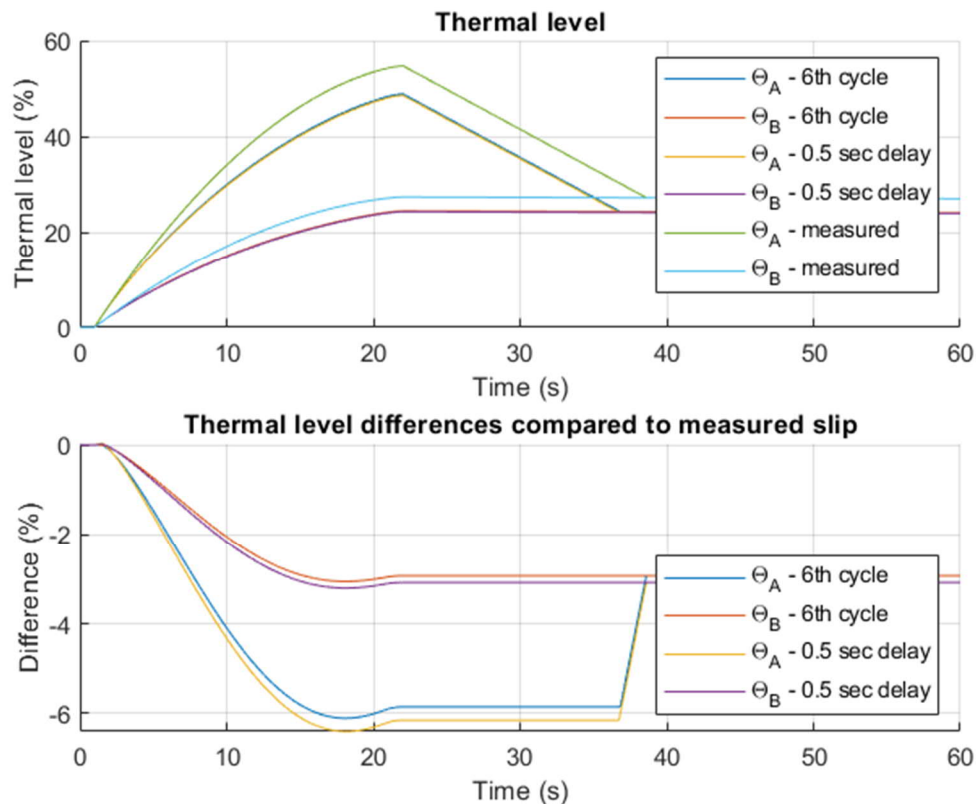


Figure 35 Comparison of the thermal levels of the second measurement.

The slip estimate based thermal levels are identical, meaning that the initial stator resistance also has close to identical values in both definition methods. And even though the thermal levels differ similarly to the first measurements 0.5 second method thermal levels, the difference is small, about 5 – 6 percent.

The slip estimates of the third measurement had some fluctuations in the beginning of the start, however, the bigger difference in the thermal levels is caused by the difference between the estimated slips and the measured slip during the entire duration of the motor start (Figure 37).

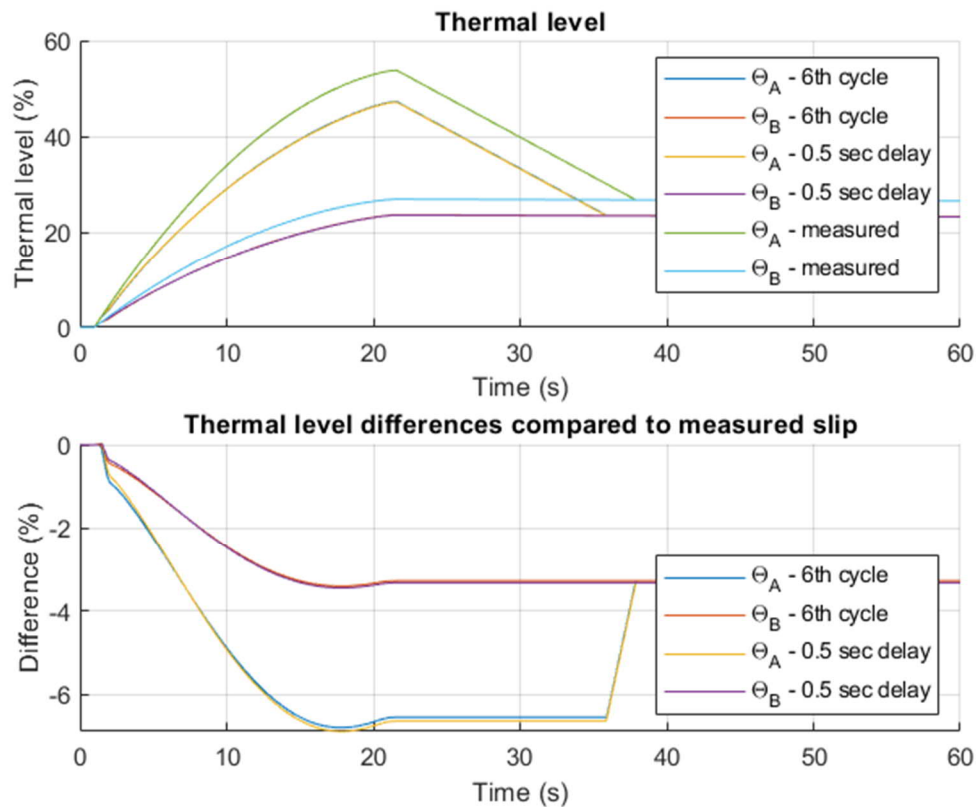


Figure 36 Comparison between the thermal levels of the third measurement.

The differences in estimated slip based thermal levels to measured slip based thermal levels are similar to the differences analyzed with the second measurement.

The thermal levels calculated with the 0.5 second method are more consistent, whereas the 6th power cycle method may result into substantial fluctuations in the thermal levels as well as in the slip estimations. Different kinds of correcting actions can be considered to be implemented for the definition of the initial stator resistance in order to make the estimated slip calculation as consistent as possible.

8 Conclusion

During the thesis work the focus in the development objectives concentrated on the first one i.e. to develop a rotor thermal model that takes slip into account. A slip estimation calculation method was found in the existing literature and integrated into the existing thermal model. The new thermal model was analyzed with PSCAD simulated data as well as with data measured from an actual induction motor.

The analysis with the simulated data gave promising results as the slip estimation was very accurately calculated. This result was repeated with the unbalance analysis. However, when investigating the performance in the condition where the CT saturates, the slip estimation became heavily fluctuated. This challenge was reasonably dealt with by giving the initial stator resistance definition more time. This way the fluctuations in the measured current could be waited out. In addition, selecting a sufficiently good CT should also answer to this challenge.

The slip estimation calculated from the measured current and voltages differed slightly from the slip that was calculated from the tachometer measured pulses. The difference was relatively small which could also be seen from the comparison of the thermal levels, the absolute percentual difference being only about 5 percent.

Based on the analysis made, the developed thermal model could be utilized to improve the existing ABB motor thermal protection by providing a more accurate thermal protection for the rotor and allowing the locked rotor condition to be detected without a separate speed measurement. This will provide better protection especially for high-inertia and ATEX-rated motor cases.

The development of the new rotor thermal model will continue as there are potential simplifications that would also enable the slip estimation to be more accurate. Also, more measured data is expected to be obtained in order to investigate the slip estimation calculation more as well as test it for synchronous motors with induction starting.

References

- ABB Oy. (2019). Relion Protection and control, REX640 Technical Manual. <https://new.abb.com/medium-voltage/distribution-automation/numerical-relays/multiapplication/protection-and-control-rex640>
- Bazurto, A., Quispe, E. & Castrillon, R. (2016). Causes and failures classification of industrial electric motor. https://www.researchgate.net/publication/313296576_Causes_and_failures_classification_of_industrial_electric_motor
- Baradkar, M. (2018). Slip ring Induction Motor, How it works ? <https://www.learnengineering.org/slip-ring-induction-motor-how-it-works.html>
- Blackburn, L. & Domin, T. (2006). Protective Relaying, Principles and Application, Third Edition. Taylor & Francis Group, LLC.
- Herman, S. L. (2011). Alternating Current Fundamentals. <http://online.anyflip.com/xetl/eids/mobile/index.html>
- International Electrotechnical Commission. (2013). Measuring relays and protection equipment – Part 149: Functional requirements for thermal electrical relays (60255-149). International Electrotechnical Commission.
- Korpinen, L. (1998). Sähkövoimatekniikkaopus. http://www.leenakorpinen.fi/archive/svt_opus/
- Pacific Gas and Electric Company. (2009). Voltage Unbalance and Motors. https://www.pge.com/includes/docs/pdfs/mybusiness/customerservice/energystatus/powerquality/voltage_unbalance_rev2.pdf

- Pyrhönen, J., Jokinen, T. & Hrabovcová, V. (2014). Design of rotating electrical machines (Second edition.). Chichester, West Sussex, United Kingdom: Wiley.
- TECO-Westinghouse. (2019). Wound rotor. <https://www.tecowestinghouse.com/PDF/woundrotor.pdf>
- WEG Group. (2012). The ABC's of Synchronous Motors. <https://static.weg.net/medias/downloadcenter/hfe/hf4/WEG-the-abcs-of-synchronous-motors-usaem200syn42-brochure-english.pdf>
- Whatley, P., Lainer, M., Underwood, L. & Zocholl, S. (2008). Enhanced Motor Protection With the Slip-Dependent Thermal Model: A Case Study. <https://doi.org/10.1109/CPRE.2008.4515056>
- Wikipedia. (2020). Stator. <https://en.wikipedia.org/wiki/Stator>
- Zocholl, S. (2010-3-9). Motor protection using accurate slip calculations (US007675720B1). Google patents. <https://patentimages.storage.googleapis.com/ad/78/85/87d329f20909b0/US7675720.pdf>
- Zocholl, S. (2007). Optimizing Motor Thermal Models. <https://doi.org/10.1109/ICPS.2007.4292097>
- Zocholl, S. (2003). AC Motor Protection. Schweitzer Engineering Laboratories, Inc.
- Zocholl, S. (1990-4-3). Method and apparatus for providing thermal protection for large motors based on accurate calculations of slip dependent rotor resistance (US4914386A). Google patents. <https://patentimages.storage.googleapis.com/36/60/e9/5029288526b9a0/US4914386.pdf>